POLITECNICO DI TORINO

MASTER's Degree in Civil Engineering

MASTER's Degree Thesis

Green Roofs as an alternative solution for stormwater management in Turin, Italy

Supervisors

Prof. FULVIO BOANO

Candidate

SAMUEL HENAO PEREZ

OCTOBER 2024

Abstract

Urban stormwater has been increasing significantly in recent years due to drastic changes in climate and the environment as a result of the expansion of paved surfaces. In highly urbanized areas, where impermeable surfaces dominate, surface runoff can lead to frequent flooding and bring serious challenges for stormwater management. Green roofs have emerged as an effective strategy to mitigate stormwater runoff while offering additional ecological benefits. This thesis examines the hydrological performance of green roofs under historical and future climate scenarios, over a 65-year projection, in four different cases under identical meteorological conditions for the city of Turin, Italy. Climate data, including historical observations (1981-2006) and future projections based on the IPCC RCP 4.5 scenario (2006-2070), were obtained from the Euro-Mediterranean Center on Climate Change (CMCC) as part of the Highlander project, which employs convection-permitting regional climate models (CP-RCMs) at a spatial resolution of approximately 2.2 km. These models are particularly innovative due to their ability to simulate convective precipitation at an hourly timescale, making them highly effective for assessing future climate impacts.

The Green Roof model analyzed features a surface area of 16 m^2, with a multilayered structure comprising a total thickness of 19 cm, of which 9.5 cm is a loamy soil substrate. With a soil porosity n of 0.43, the active soil depth (nZ_r) is approximately 40 mm. The analysis evaluates three vegetation types: sparse succulent, dense succulent, and herbaceous, by varying the crop coefficient (K_c), and in one scenario, doubling the active soil depth (nZ_r) to assess its impact on runoff reduction. Results indicate that vegetation with a higher crop coefficient ($K_c = 1$) leads to increased effective evapotranspiration and a corresponding reduction in runoff. Herbaceous vegetation, in particular, was found to reduce runoff volume by 12% compared to sparse succulent vegetation. When doubling the active soil depth (nZ_r) further reduces runoff by 11%, attributed to the increased water retention capacity of the system. These findings provide valuable insights into optimizing Green Roof designs for improved stormwater management in urban areas.

Acknowledgements

With this thesis my academical journey in both Universidad EIA and Politecnico di Torino, comes to an end. I would like to start by thanking the universities for the high-quality building they provided me with and also for all the tools, the friendships, the experiences and the learning I acquired during these years as a university student.

My deepest gratitude to my academic tutor Professor Fulvio Boano, for his support and guidance in this process. I also want to highlight his precision, dedication, and teaching style, which were the reasons I initially asked him to be my supervisor.

I would like to thank all my family for always supporting me. They encouraged me to pursue my dreams by coming to Italy and have been there for me ever since from the distance. A very special acknowledgment to my parents, my sister and my grandfather, who from the very beginning encouraged me to come to go abroad and believed in me. For them, and also for Juanita, my warmest thanks for their support during challenging times and for always encouraging me unconditionally.

A special thanks also goes to all my friends who, despite the distance, have been a great source of support, as well as those I met during my Master's in Turin, who have shared this journey with me.

Table of Contents

List of Tables

List of Figures

Chapter 1

Introduction

In recent years, a lot of variations in the environment are emerging and bringing with them a considerable amount of new challenges. Mainly in the urbanized areas, where the landscape has been strongly reshaped and intervened by man. One of those challenges is the management of the stormwater that falls in these areas and cannot infiltrate directly into the soil as before, due to the presence of all kinds of infrastructures that either decrease or totally remove the permeability of the soil and force the water to find other ways to the water courses. For stormwater one understands the melting snow or the rainwater that does not get absorbed by the soil and runs off into waterways. In the cities it flows from the roofs, streets, paved areas and sloped terrains, taking all kinds of materials on its way to the watercourse.

According to the book Sustainable Cities and Communities, stormwater is defined as “all rainwater or melted snow and hail that runs off pavements, streets, lawns, and other land surfaces and did not infiltrate into the soils or other permeable surfaces” [1]. The significance of stormwater lies in its potential to contribute to flooding and other natural hazards, particularly in urban areas. It further emphasizes that excessive surface runoff is largely attributed to the combination between extreme meteorological events and land use practices in urbanized settings, where impermeable surfaces limit natural infiltration and increase flood risks.

Out of the different sustainable solutions proposed for stormwater management, Green Roofs are being strongly investigated in the last years. Emerging as a promising nature based solution in the paved areas, they are presented with other benefits more than the flow attenuation capacity. Mainly, Green Roofs contribute to reduce the so called "heat island effect" in the cities and provide thermal insulation for the buildings in both cold and hot environments reducing the thermal flux. Being a good alternative for recovering green spaces in cities, Green Roofs bring also advantages in terms of the amenity for the people and the biodiversity [2].

As stated in the Strategic Plan for Green Infrastructure presented by the City

of Turin in [3], this city is facing, like any other city around the world, the changes in climatic conditions. Emphasizing the increase in temperatures, the frequency with which the most intense extreme events will occur and the reduction in the number of rainy days. It highlights the need of the city to start creating mitigation solutions to these extreme events, by adapting them in a more sustainable way. The Plan for Green Infrastructure also refers to the Climate Resilient Plan where ARPA Piemonte made a vulnerability analysis and focused attention on the increment of days with intense rainfall [4]. Furthermore, it states that due to these concentrated rainfalls in short periods of time, the soils in the hills are presenting a detrimental impact, mainly in places with already unstable conditions.

The goal of this study is to analyze the effectiveness of green roofs as a potential solution for stormwater management in urban areas, with a specific focus on reducing flooding events. This will be examined through a case study in Turin, northern Italy. Furthermore, the Green Roof reaction to both historical and future scenarios will be contrasted to determine the best option out of four cases for the reduction. It is important to mention that these cases have variations in the type of vegetation and the thickness of the soil layer.

Chapter 2

Theoretical Framework

2.1 Stormwater

In recent years, numerous environmental variations have emerged, bringing new challenges, particularly in urbanized areas where human intervention has significantly reshaped the landscape. One of these challenges is managing stormwater, which can no longer infiltrate the soil as before due to the presence of various infrastructures that reduce or eliminate soil permeability. Consequently, stormwater must find alternative routes to watercourses. Stormwater encloses melting snow and rainwater that the soil cannot absorb, leading to runoff into waterways. In urban settings, it flows from roofs, streets, paved areas, and sloped terrains, carrying various materials into watercourses.

Specifically, the book "Sustainable Cities and Communities" defines stormwater as “all rainwater or melted snow and hail that runs off pavements, streets, lawns, and other land surfaces and did not infiltrate into the soils or other permeable surfaces. Stormwater is of special concern because of its potential to cause floods and natural disasters” [1].

The author also notes that excess overland flow results from the combination of extreme meteorological events and land use issues in urbanized environments.

2.1.1 Stormwater Management

The management of the stormwater has been a matter of importance for societies since ancient times. Understanding how to manage the quantity and the quality of water that falls after a rainfall event are the two key elements. Stormwater transports on its way a lot of pollutants that collects from the surface, becoming a sanitation problem, mainly in the urbanized areas. That is the reason, a lot of care is needed when managing the water, meaning good systems that prevent contamination or overflow of pipes, causing sewage to rise to the surface. Regarding

this aspects, there are two types of managing water sewage, it can be combined or separated. The combines consists on a unique pipe that transports the wastewater together with the surface runoff to the Wastewater treatment plant (WWTP).

In recent years, there are emerging new alternatives to asses the stormwater management in both urban and rural areas. One of this terms is the Best Managing Practices for stormwater (BMPs), which refer to devices, methods or applications that are used to control the peaks of runoff from the stormwater. These are also divided by their land use and whether they are structural or non structural, the last two referring to the mitigation or reduction and to the planning and design of the practices [5]. Furthermore, other ways to characterize them is by their maintenance and if they are green infrastructure.

The traditional way sewer systems began being changed in the past years, by increasing the space below the ground for create detention and reducing the floods in the paved urban areas. Nevertheless, that solution is not enough, so alternatives need to be found. Here is where the Sustainable Urban Drainage Systems (SuDS) appear. Its aim is to help with water disposal and also to create sustainable and greener environments within cities, not only by reducing the flooding and creating retention basins for the excess water inside the cities, but also in terms of water quality. These types of structures help function as natural filters [6].

2.2 Sustainable Urban Drainage Systems (SuDS)

As a result of the industrialization and the continuous development of the cities, the green areas inside them started to be more limited and the impermeable surfaces (such as concrete) began to predominate in the urban landscape. Together with this comes the issue of management of the water that falls to the surface in the form of rain and must continue its way to a water course and infiltrate some part of it, so the water cycle is not affected. The appearance of the impermeable structures inside the cities causes that the water that falls on them does not get absorbed or infiltrated, instead it turns into water runoff. In case of a big rainfall event, this runoff water can evolve into a flood and cause several repercussions inside the city and to its inhabitants. This is when the alternative of creating sustainable urban drainage systems appears, bringing with it more advantages than only managing the runoff water[2].

2.2.1 The Design process of SuDS

SuDS tend to manage the surface runoff in the best possible way. their design process depends on the necessities of each particular case and also the available space for the possible solution. To do so, there are four main pillars for which

these type of structures are design: water quality, water quantity, Biodiversity and Amenity. Their principal goals are summarized in Table 2.1.

SUDS Category	**Objective**
Water Quality	Manage the quality of the runoff to prevent pollution.
Water Quantity	Control the quantity of runoff to: • support the management of flood risk. • maintain and protect the natural water cycle.
Biodiversity	Create and sustain better places for nature.
Amenity	Create and sustain better places for people.

Table 2.1: Design objectives of each SUDS category[2].

Water Quality

For the water quality management, one understands that the pollutants must be removed or at least reduced to certain levels where they do not affect the health of the consumers, mostly when the water is going to be in touch with something related to the human consume. In ordinary urban drainage systems, the pipes are designed to not let the particles settle inside of them, so all the pollutants end up in the receiving waters. Even though some catchment structures have filters to prevent sediment of going into the pipe, their performance depends on the maintenance they get. There is where the SuDS appear, they can catch and clean the surface water, so it gets clean into the receiving environment. Many of those pollutants can be influenced by the drainage path, the duration and intensity of the rainfall event, the duration of the precedent dry period before the rainfall event, among others. Furthermore, the general impact on the receiving waters can be measured in terms of the types of pollutants, the peak pollutant concentrations and the total pollutant load. [2] To better understand the loads and the pollutants concentration one can have after a rainfall event, one has to know that at the beginning of a meteorological event there is a peak "flush" of pollutants. Usually in considerably small precipitation events one can get a very high initial pollution concentration.

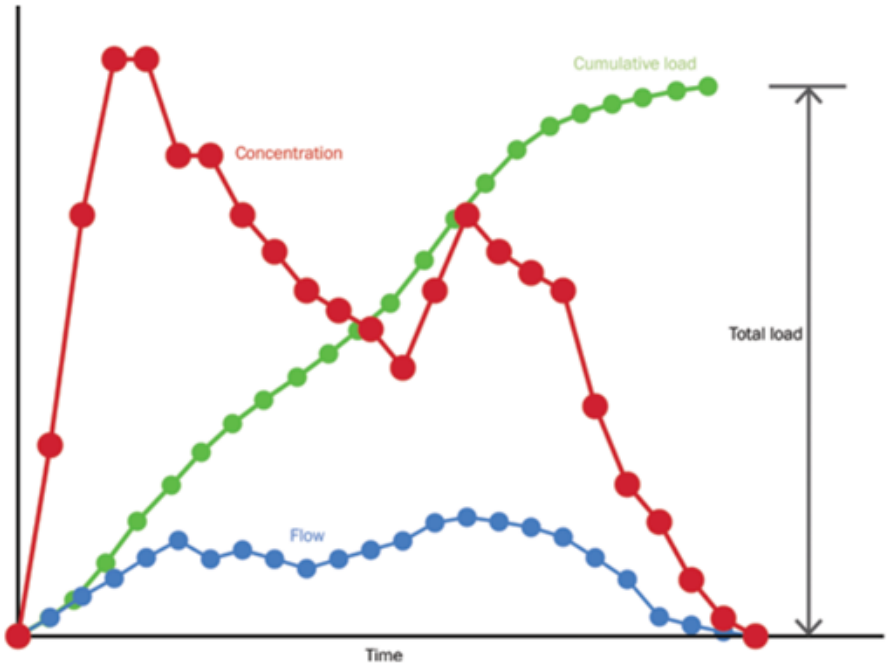

Figure 2.1: Flow, pollutant concentration and pollutant load graph [2].

In Table 2.1 one can see the goals of the water quality in the design of the SuDS, but when referring to the design criteria for the water quality, one has: the support in the management of the water quality in the receiving surface water and in the underground waters, as well as the resilience of the design system, so it can cope with future challenges. To sum up, the aim of the water quality design criteria is to return to the environment the water in good sanitary conditions and maintain clean the water that is already stored in natural aquifers or groundwater and do not let it get affected by the surface pollution, as well as to manage the surplus runoff.

Water Quantity

When designing the water management capacity of Sustainable Drainage Systems (SuDS), it is crucial to prioritize flood risk management and the preservation of the natural water cycle. This includes maintaining control over peak runoff rates and total runoff volumes through various strategies. Among these strategies, SuDS play a significant role in preventing riverbank erosion due to their retention capabilities and ability to reduce the time to peak discharge. SuDS are particularly effective in mitigating flood risk for events of short to medium duration, as longer-duration events typically set risks related to flooding in the nearby areas of the rivers. Consequently, SuDS are predominantly utilized in urban areas, where they are

instrumental in controlling flow rates and volumes, thereby reducing local flood risk.[2] The SuDS Manual underscores the importance of implementing SuDS in conjunction with other sustainable drainage systems. It has been demonstrated that SuDS exhibit superior performance when deployed as part of a collective system rather than in isolation. The cumulative effect of multiple SuDS in each area is essential for achieving significant, visible improvements in flood risk management and setting important precedents. One effective approach to controlling peak discharge following a substantial precipitation event is to attenuate the post-development runoff rate to match the pre-development rate. This concept, which focuses on slowing and storing runoff, is illustrated in the Figure 2.2. [2]

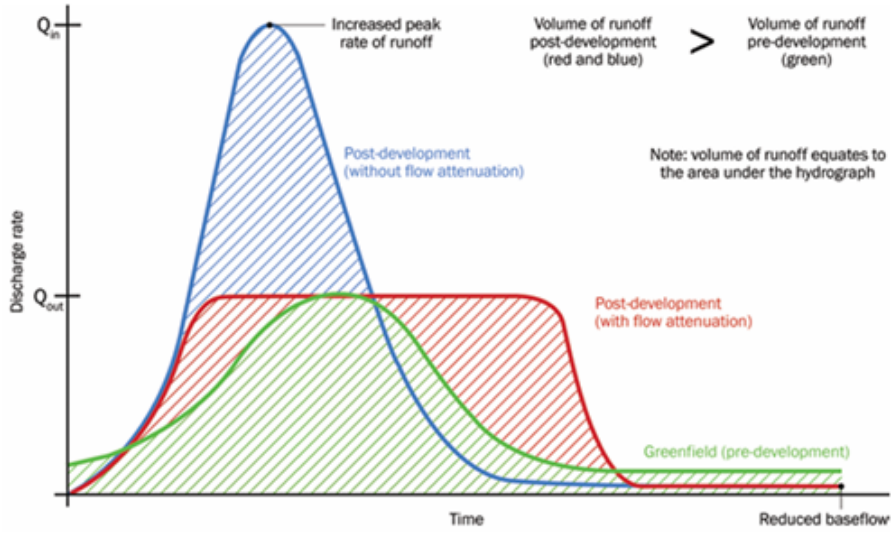

Figure 2.2: Runoff hydrograph [2].

Regarding attenuation, it is fundamental to control the changes in the volumes, so the hydrograph is kept constant, and flooding is avoided. As said before, this process of attenuation is more visible while having a larger group of SuDS together and not only one small system on a specific area. In this process some of the design criteria of the water quantity can be followed. For example, the use of the runoff for other purposes, protect and preserve the hydrological systems on the area, efficiently sink water from the area, among others. Specifically, for this purpose the one that interests the most is the control peak runoff rates from the site. Keeping in mind that managing the water runoff helps prevent high rates and volumes. In terms of design standard, the drainage system should be designed to ensure that the peak runoff rates during severe rainfall events are maintained at the natural, undeveloped (greenfield) runoff rates for the same event [2].

Biodiversity

The design of SuDS is a multidisciplinary task that involves professionals from the engineering sector, the landscape design sector and ecological sector. It aims to bring benefits by introducing different types of plants in new and old habitats (that get reconstructed), depending on the site necessities. Also, looking to preserve, support and protect the habitats and their species. As mentioned above, the SuDS function more efficiently as an integrated system than when they are implemented independently. A good way of doing so is to take native species that hardly grow nowadays in the city, because of urbanization, back to a protected area that is pleasant for the observer's view and safe for the nature to grow. This comes by the hand of the European initiatives to preserve and protect certain species and habitats. Another plan of action in these cases is to reconstruct some habitats that previously worked as connections between habitats, such as green corridors or certain green roofs that contribute to the species to have an easier migration along the urban landscape [2].

Amenity

In order to keep a balance, a good design takes into consideration how attractive, how pleasant and how useful will the SuD for its surrounding community. These alternatives for water management on the surface bring with them many benefits like the decrease in temperature during the summer, what comes also together with the idea of avoiding the heat islands inside the city. This also comes with the option for some species (both fauna and flora) to have a habitat back. Furthermore, it can also be seen as an opportunity for the education of the community in terms of caring for the environment and exploring other green solutions for the challenges that the society faces with the management of water as well as the importance of the preservation and care of the water cycle. The amenities cover a very wide landscape and have many benefit fronts such as air quality, biodiversity, ecology, reduction of carbon emission, economic growth, education, noise reduction, health and recreation, among others. It is important to consider that depending on the local situation, the design criteria may vary and bring with them the certain benefits that the community needs. [2]

As design criteria, the main one could be the maximization of the multi-functionality, where the landscape architects have to work together with the drainage engineers, so they obtain a well-achieved result. Other very important criteria is the adaptability or the resilience that the system need to have after its design and construction to face future changes in the environment and the culture. It needs to guarantee that it will be able to manage the received precipitation as well to help with the needed climate resilience regarding the expected drastic changes on the temperature. Nevertheless, is good to mention that the designer

should guarantee that human interaction with this type of structure is safe and will not affect people's health. For example, places where rainwater can be exposed to some type of pollutant or contaminant that is bad for human health. Furthermore, the idea of the good introduction of the SuDS into the urban landscape aims to give the community tranquility and a place to enjoy, which is also achieved visually and makes aesthetic design play a key role. [2]

2.2.2 Types of SuDS

The technology advancements have shown that there are many different solutions to assess stormwater. The key point is to identify which of them is the optimal solution for the specific problem that one needs to solve. In following some of the the different types of SuDs are listed, which are described on a technical way on the SuDS Manual[2]:

- Rainwater harvesting.
- Green Roofs.
- Infiltration systems.
- Proprietary treatment systems.
- Filter strips.
- Filter drains.
- Swales.
- Bioretention systems.
- Trees.
- Pervious pavements.
- Attenuation storage tanks.
- Detention basins.
- Ponds and wetlands.

2.3 Green Roofs

The origin of Green Roofs goes back many years, even some centuries before Christ. They started as a solution to preserve the temperature inside the homes or in the early shelters, where the people needed protection in order to survive. To do so, in the Neolithic, they started to build dwellings below the land surface. Those dwellings or shelters started to have the earth as a daubing layer that allowed to create an impermeable layer, that with the roots growth assured the creation of a meadow roof. This type of roof can be said that is the ancestor of the Green Roof, creating isolation in the inside and maintaining the temperature of the inside environment facing the extreme weather conditions they had to live in.[7]

Figure 2.3: Example of Icelandic Turf Houses.

The evolution of the dwellings or shelters were the so called "Turf or Sod Houses" that were mostly used in the Nordic European countries in the medieval times and in North America in the early modern times. Those houses were built with stones and hood and then covered with grass sods of a significant width, in order to face the harsh weather they had to face. This type of houses were very common in Iceland, and one can see an example in Figure 2.9 [8].

In other regions of the world, they also used vegetation on the roofs as a kind of an ancient green roofing. An example of that is in Pompeii, where there are clear signs that the city was built with a lot of green spaces and there is a specific house,

"Villa dei Misteri", where there are traces of a hanging garden in the House's and also evidence of a vegetated roof. Since the end of the 1800s in Germany, green roofs were improved by the need of a housing problem due to the industrialization of Berlin. As the factories needed more apartments for their workers, they started to construct more buildings and to isolate the roofs with tar. What they did not know, was that it was very flammable and represented a big risk for fires in the building. A roofer called H. Koch had the idea of placing a layer of a sand-gravel mixture above the one of tar and so protect it of catching fire. In that layer of sand and gravel, vegetation started to germinate, due to the porosity of the materials and their capacity of retaining rainwater. That vegetation, which at the beginning was seen as an invasive species, was then pleasant and well accepted by the community [9].

In the first half of the 1900s, the evolution of green roofs started to appear in famous infrastructures such as the Rockefeller center in New York City (1939) or the Monastery of La Tourette in France (1953). It was in the 1960s when the green roofs were used in Germany as a new design of a light weighted green roof [10].

In the decade of the 60s the subject of Green Roofs started to sound due to the need of a modernization of the subject. Primarily, the use of green roofs emerged as a strategy to optimize and utilize space, especially in highly urbanized areas facing challenges with stormwater management. These structures offer numerous benefits to the buildings on which they are constructed, notably by reducing surface runoff, providing ecological value, and enhancing thermal regulation by improving the building's internal temperature control. It is important to note that green roofs are categorized into two types: extensive and intensive green roofs. The main distinction between these two, aside from their size, is the thickness of the green layer, which directly affects the load transferred to the structure[2].

2.3.1 Design of Green Roofs

When designing a Green Roof there are several aspects to consider. Mainly is important to know how much water is going to be discharged from the roof as an excess from the precipitation that does not get absorbed by the vegetation or evapotranspirated. Starting from the Hydraulic design, one needs to know how the structure will react to an extreme event and also how is going to behave in the course of the year. Is also very important to mention that the performance in terms of absorption of a Green Roof depends mainly on the previous conditions, meaning the soil moisture, the temperature and the mm of precipitation from previous days. To be able to assess this, one needs to have an extensive time series of observed and scenario data, so one can model the behavior of the green roof and have an idea of how its performance[2]. From a hydraulic point of view is important to know the peak flow control design, the volume control design and the exceedance flow design.

Over the dry season, for small to medium intensity events, the Green Roofs have a very good performance regarding the peak flow control design by reducing and attenuating the generated runoff. The volume control depends principally on the type of vegetation used on the roof and the season of the year; well, it is known that Green Roofs reduce the runoff in warmer periods when the soil moisture is minimum. In addition to that, is also very important to consider a possible case of failure, when the design event gets surpassed and the actions that will be taken in that possible situation[2]. Also, as it was mentioned in subsection 2.2.1, the amenity and the biodiversity design have to be considered and analyzed to improve the ecological value and the benefits beyond the technical field[2].

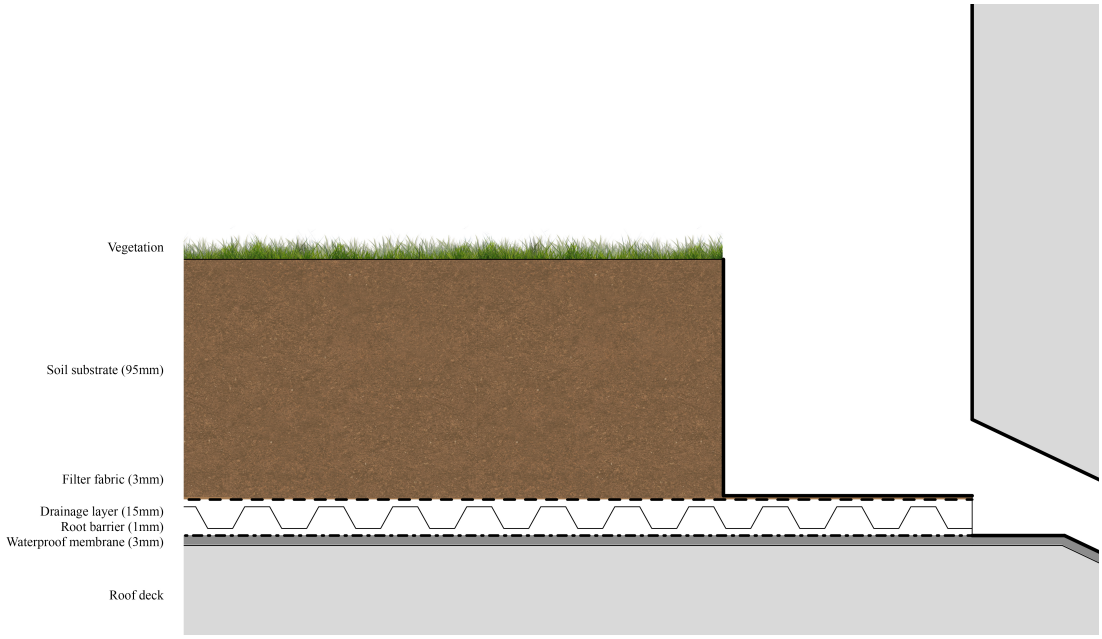

Figure 2.4: Cross section showing the components of a Green Roof[2].

In figure 2.4 it is possible to see the cross section of a typical Green Roof. Those are the main layers that the roof has to include and also there are some physical specifications that need to be met. They need to be fire resistance, where all the vents and openings need to be surrounded by non-vegetative materials that avoid the spread of the fire in case of one and need to be designed according to the local building regulation. Furthermore, the Green Roof needs to have an inclination whether they are over a completely flat surface or over an already inclined one, they need to have a slope to guarantee the flow of the water. Also, on very steep roofs, there needs to be assured that there is no erosion of the material and vegetation and that the Green Roof structure is well attached. Other aspects need to be considered, such as the irrigation systems, the access to the roof in case of maintenance and also

the outlets of the buckets connecting to the water downspouts[2]. Regarding the roof supports and the loads transferred from the green structure to the building, are on a range from $0.5 - 5\frac{kN}{m^2}$ depending on the type of Green Roof and the vegetation it contains. The distributed load is accounted for the saturated soil, and in case of a storage layer, with the content of the full storage layer. And the live loads will still be for the workers that come for the maintenance of the roof or in some cases, if the roof is walkable, for the people visiting it. Another important aspect is the wind load, that in this type of roofs is approached in the same way as ordinary roofs are, so in the corners of the roof, where there is more uplifting pressure, no vegetation can be placed[2].

2.3.2 Examples of Green Roofs

Giving a closer look to the evolution of green roofs around the world, one can see the approaches that various cities took to become more sustainable and increase the green coverage. Most of them started with the idea of giving the empty or partially empty roofs another function apart from the use of the cooling system placement or the storage of some type. For this part, the evolution of the modern green roofs will be divided by continent and then, into the most remarkable cities on this field. Also, others had the idea of renewing old infrastructure and give it a new use, for example roof gardens or parks for the amusement of the citizens.

Europe

- London:

  It was in 1938 when the first roof garden was installed on top of a store in the Kensington neighborhood, in the heart of London. The green structure had a surface of 6000 m^2, being Europe's largest roof garden for a considerable time. Furthermore, it is an example of the durability of these structures, because even though the store closed in 1973, the garden still exists in the same building, but under the ownership of Virgin. The structure consists of three different gardens, divided by landscape genres, with various types of trees and a rich vegetation. Regarding the type of construction, it counts also with a bitumen waterproofing base. Above it, one finds a loosely laid brick and rubble fragments level that form the drainage layer. Is important to mention that this layer includes a fan-shaped pipe-drain system that takes the water to an outlet. On top of these layers, one finds multi-course growth media for the vegetation with a thickness of 90cm to guarantee space for the tree's roots. Back in the 1930s there was not much information about this type of roofs and either about the self-sustainability concept, so the garden irrigation was performed with water gained from an artisan well located bellow the building.

Figure 2.5: Kensington Roof Gardens in 2017

Figure 2.6: Sketch of the original Roof Garden [11]

In recent years, the roof gardens became more famous in London. Mostly because they started to be placed on top of the skyscrapers around the city, like the one located in an office tower at 20 Fenchurch Street. This garden is the biggest one located on top of a skyscraper, with a vegetated surface of about 1500 m^2 and a panoramic view of the city. This new roof gardens are being used to create a type of enclosed environment, giving an alternative solution for keeping this type of vegetation along the whole year considering the British tough weather.

- Paris:
  One of Paris most famous green roofs is the Atlantic Garden, located above the Gare Montparnasse train station and finished in 1994. This park is located 17m above the ground of the train station, specifically over the railway tracks. It is all supported by 12 pillars of a considerable size and respective long span arches. The park came out as a solution to the urbanization of the city and the alternative of creating a park for that specific neighborhood, given that the park has children's playground, tennis courts, theme gardens, among others.

  Another structure that was renovated into a type of roof garden was the Coulée Verte, which was an old railway viaduct that crossed above 4.7 km inside the city and was abandoned in the late 1960s. This project created a park of 65000 m^2 with a bunch of different vegetation, trees and also fountains that gave life to the abandoned structure.

- Darmstadt:
  In the beginning of the new century, the architect Hundertwasser designed

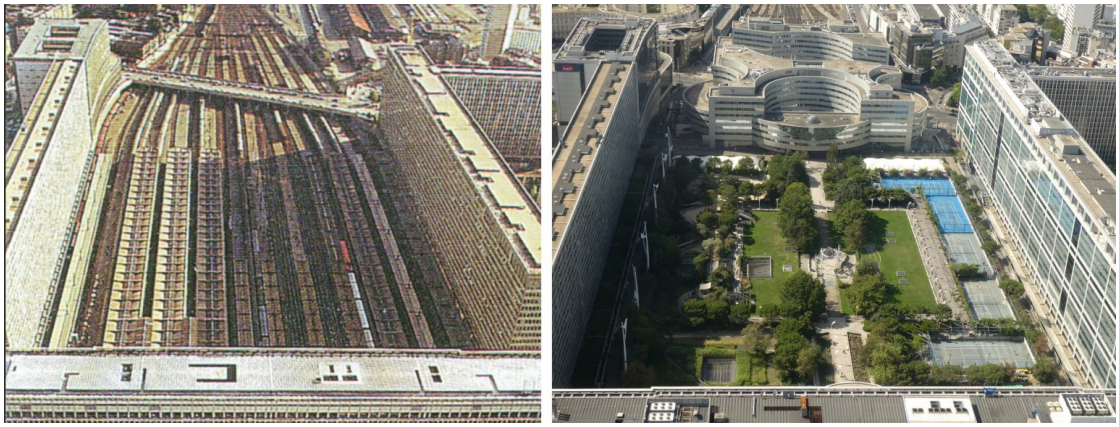

Figure 2.7: Jardin Atlantique before and after[12].

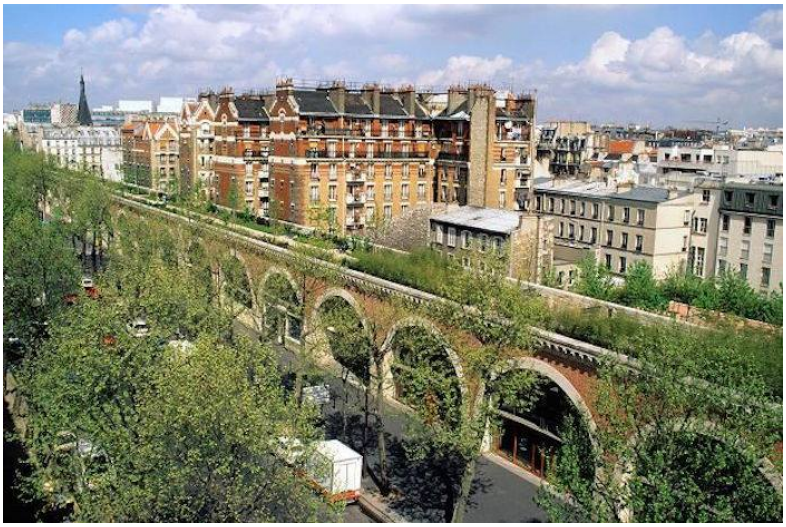

Figure 2.8: Coulée Verte [13]

a U-shaped building in Darmstadt. This building had the peculiarity of an increment on the height of the building from one side to the other, what created a roof with a slope difference because the roof was a big, bonded ramp. The roof has a surface of 3800 m^2 going from the ground level to 12 stories building, with a length of 174 meters.

- Munich:
  Back in 2004 the city of Munich opened a big new park, that like most engineering solutions, was the result of a notable problem. In fact, the new "Peutel Park" wanted to mitigate the noise that a high-capacity road emitted on the urban area and the need of the city for a new urban park. The city

Figure 2.9: Wald-Spirale in Darmstadt [14]

came with the alternative of covering the road with a deck and placing a green roof on top of it that would be used as a park. The green roof had all the properties of isolation that the city needed as well as the advantage of bringing a park to the city, without the need to remove the road. The 650 meters by 60 meters concrete roof enclosed the road (that had already an altitude depression), giving space to a new green space in the city.

As the first solution, in 2010, the city decided to do a similar project over some railway tracks, to offer a new green space of 16800 m^2. In this case, there was already an existing concrete deck, but with limited bearing capacity to resist a soil layer plus vegetation and live loads. The structure was elevated to a certain point, which was safe for the health of the people due to a risk with the electromagnetic flux that the railway operation required. In the raised structure, light-weighted elements were used as well as a Styrofoam for the core and a type of rubber paving for the surface.

America

Other examples for the use of green roofing were found in a couple of cities in America. And in this part, some of the notable solutions per city will be related.

- New York City:
  It was in the late 1800s when Americas first roof garden was opened in New York City. The aim of having a theater garden as the ones in Europe and

the elevated costs of the land in the city, resulted in converting the roof of the Casino Theatre in Broadway into a roof garden with some flower beds and a café, even though it was no more than a rooftop with some flowers in pots and small beds. This project was a reference to other types of buildings to open their roofs and turn them into gardens. That's why the New York Times called NYC the city of roof gardens in 1893.

The first prominent roof garden appeared in 1936 on top of the adjacent buildings on both sides of the main tower in the Rockefeller center in Manhattan's diamond district. These green roofs used obsolete technology for nowadays, with heavy drainage and substrate layers. That specific green roof is part of the few remaining conventional green roofs in North America, and considering the two building, they have a total green surface of $7000m^2$.

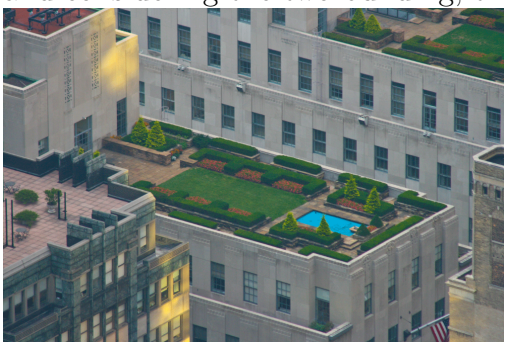

Figure 2.10: Rockefeller center roof gardens [15]

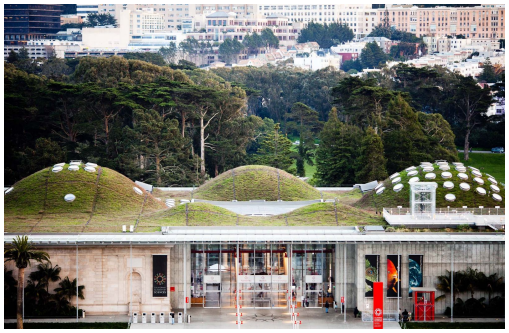

Figure 2.11: The California Academy of Science [16]

- San Francisco:
  Regarding historical reference, the city of San Francisco had the first urban park built above a reinforced underground structure. It is the famous Union Square Park that below of it counts with 1700 parking lots distributed in four stores of underground structure. The structure has 160 huge columns that support the five stores, including the park on top of it and considering it as a roof garden with a green area of 11000 m^2.

  A prominent green roof was built in 2008 in the city on top of the modern museum "The California Academy of Science" in the Golden Gate Park. One of the characteristics that make this green roof remarkable is that all the plants were placed above 50000 porous trays fabricated with biodegradable coconut oil, allowing the roots to grow through them and this organic layer that counts with 7.5cm of thickness, offers a very good thermal insulation and evapotraspiration cooling. The reduction of the inside temperature is around 5.5° Celsius and this layer works also for the noise isolation inside the structure. This structure is designed to capture most of the storm-water that

falls into the roof and reduce the storm-water discharge, improving the water quality as well due to the filtration process in the organic layer.

- Chicago:
  After an extreme heat in 1995, the City Hall of Chicago decided to renew the building's roof to turn it into a green roof to guarantee thermal isolation. In total, the roof has 3600 m^2., but only 1900 m^2 were used to install the green roof structure. As the structure was constructed in 1911, it was tested and resulted on being strong enough to support the load of a green roof. The whole project also counted on a pilot part to test the materials, its performance and the maintenance needed. The Chicago project was a pioneer in planting different species, and it served as a reference for the type of vegetation used in this kind of structure as well as the management rules that needed to be used.

  The city of Chicago became a reference when speaking about green roofs in the United States. One of the big examples in the city is the Millennium Park, that is a 100000 m^2 green space located on the roof of a subterranean car parking with capacity of 2126 cars.

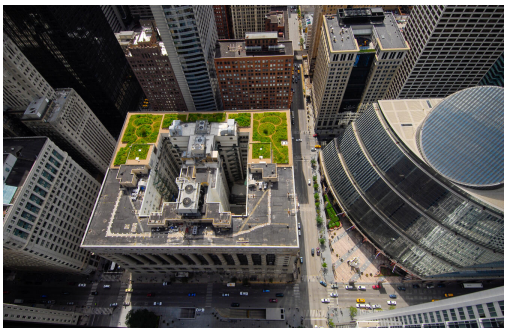

Figure 2.12: Chicago City Hall [17].

Figure 2.13: Ford River Rouge Factory [18]

- Dearborn, MI:
  On top of the Ford River Rouge Factory was built the biggest Sedum roof in the world. The construction was done in the year 2000 over the new truck plant, with an extension of 42178 m^2. It is vegetated by succulent plants that lay above a 3.2 cm mat system that is light in weight so the whole structure can get saturated and arrive to a wight of 49 kg/m^2. The thermal capacities of the green roof help to maintain the indoor temperature of the factory 5.6řC below the outside one during summer, and 5.6°C above the outside temperature during winter. Furthermore, it helps in the reduction of storm-water discharge, as the system has a great capacity of retaining the water and helps to improve its quality.

Asia

- Tokyo:
  It wasn't until the 1980s when the green roofs started to be a reference for this type of structure in Japan. One of those is the roof garden placed on top of the Mitsui Sumitomo headquarters in the Kanda-Surugadai district. The building was constructed with a U form, that provided $2600m^2$ covered with dense woodland in most of that area. In the remaining part, the company decided to reserve it for the installation of a community garden. The nearby neighbors had the right to participate in a raffle, so they could get a slot to cultivate on the small crop for one year. With this initiative, the company wanted to include the community and to profit from the benefits of a woodland such as the air quality, the reduction in the inside temperature during the summer and the mitigation of the urban heat island effect in cities so densely populated.

Figure 2.14: Mitsui Sumitomo headquarters [19].

- Fukuoka:
  In 1995 the Asian Crossroads Over the Sea building was finished with the impressive combination of a green roof and a green wall. It resulted in creating a large, stepped garden covering the whole building facade. Each of the terraces has a organic layer with thicknesses between 30 and 60 centimeters. The total green covered area of the building is 8300 c, becoming the building with the largest green cover in the world.

- Osaka:
  In this city, back in 1996 the first green roof on top of a sports structure was placed. The structure is the Municipal Central Gymnasium in Yahataya Park that consists of two stadiums, where two green roofs were installed with areas

Figure 2.15: Asian Crossroads Over the Sea building [20].

of 14500m^2 and 2500m^2. A very planned installation of the vegetation took place, so the position of the trees do not affect the load bearing capacity of the structure. The idea of the installation of this roof was to return nature to the park, where both stadiums were constructed and to mitigate the heat that the bare roof created inside the sports center.

- Hong Kong:
  This is one of the cities in the world that faces the most the problem of a big population density with not so much space, resulting on a public space provision of 2,9 m^2/person. And in 2005 the University of Hong Kong started to evaluate how to mitigate this problem with the introduction of green roofs. They began with the creation of a woodland on an electric substation back in 2005. Some other buildings imitated the same type of green roof, but in 2008 the intervention performed on another electricity substation did not stop with the creation of a 580m^2 green roof. The designer wanted to create a tropical woodland, by placing native trees on the building envelope and putting climbers on the facade. It resulted in the coverage of 900m^2 of walls with a height of 13,5m. All of this resulted in showing the flexibility of mixing the envelope vegetation with the one of the green roofs and green walls. From all of this, one can see that in the 1960s a renovated type of green roofs came, with new materials and optimized components of the roofs such as the lightweight plastic root barrier and the drainage layers in comparison to the bottleneck used in the previous exemplars of the green roofs.

2.4 Reference framework

In this part, some similar works are presented in order to have an idea of how this issue has been assessed in other regions of the world. The different projects proposed around the world are used for the later simulation of the Green Roof.

1. **Management strategies for maximising the eco hydrological benefits of multilayer blue-green roofs in Mediterranean urban areas.**

   The goal of this study was to model the hydraulic behavior of a Multilayer Blue-Green Roof (MBGR) system by adapting the eco-hydrological streamflow model (EHSM) developed by E. Cristiano, F. Lai, R. Deidda and F. Viola in [21]. A primary focus was to simulate key processes, including evapotranspiration and soil moisture dynamics within the soil layer, as well as evaporation and water level fluctuations in the storage layer.
   The model structure integrates a "soil bucket" and a storage reservoir, simulating the following process: rainfall infiltrates the soil, and once soil moisture reaches its field capacity, excess water percolates into the storage layer.
   The analysis addressed three main objectives: mitigating pluvial flooding, maintaining water reserves for domestic use, and reducing structural loads on rooftops. The model incorporates five key parameters: active soil depth (nZ_r), soil moisture content (s_t), hygroscopic point (s_0), crop coefficient (K_v), and evaporation reduction coefficient (K_E). These observations were done for a six-month period from November 2020 to April 2021, and an important aspect is that its performance was evaluated comparing the observed and the simulated water levels in the storage layer measurements.
   Two of the parameters, the crop coefficient (K_c), and the evaporation reduction coefficient (K_E), were calibrated using a Monte Carlo simulation. After the model was calibrated, rainfall time series were generated with applying a stochastic point modelling process, which is called the Newman-Scott Rectangular Pulse model (NSRP). The model wants to describe the time between consecutive events, the duration and intensity of each event.
   When referring to the maximization of the average annual stored volume, it was necessary to obtain the maximum daily average value. In this analysis, it was obtained by simulating the behavior of the green roof while the gate is always closed and considering the three time series, resulting in a value of $0.4m^3$. It is important to clarify that the maximum volume that the prototype of the study can store is $1.28m^3$.
   Focusing only on the runoff mitigation capacity, the obtained results confirm the findings presented by Busker et al. (2022), that investigated the performance of a MBGR installed in the Netherlands in retaining extreme events with different management rules. They found that if the gate is always open,

the runoff generation is reduced up to 12% and it rises to 59% if the gate is always closed. On the other hand, when the gate is regulated according to the weather forecasts, the performance increases, varying between 70% and 95%. Although the retention capacity of the Dutch prototype presents similar behavior to the Sardinian MBGR under different management rules, the performance in mitigating rainfall extremes higher in Cagliari, suggesting the high potential of this nature-based solution in Mediterranean climate.
In the R2 scenario, which represents a MBGR configuration without gate regulation, the reduction of outflow is influenced not only by the antecedent soil moisture but also by the water level within the storage layer. Under optimal conditions, when the soil is dry and the storage layer is empty, the MBGR prototype has a maximum retention capacity of 94.78 mm of water, with 15% stored in the soil and 85% in the storage layer. However, such ideal conditions are rarely achieved. In most instances, when the gate remains closed, the soil is partially saturated, and the storage layer is partially filled, limiting the retention capacity.
A key finding from this study is that short-duration, high-intensity precipitation events with extended return periods are insufficient to fully saturate the soil layer. Furthermore, the analysis indicates that maintaining the gate in an open position over extended periods results in an average reduction of annual outflow ranging from 32% to 45%, depending on the specific rainfall time series evaluated.

2. **The potential of multilayer green roofs for stormwater management in urban area under semi-arid Mediterranean climate conditions.**
The objective of this study is to assess the stormwater retention performance of a multilayer green roof, also known as a blue-green roof (BGR), using data collected over a one-year period through a network of advanced sensors. The work was presented by D. Pumo, A. Francipane, F. Alongi and L. V. Noto in [22].Various hydrological indicators are analyzed to evaluate the roof's hydrological response to different rainfall events, considering the influence of storm characteristics.
The system consists of two primary layers: the blue layer (BL), which functions as the storage layer, and the green layer (GL), which retains infiltrated rainfall. During dry periods, water stored in the BL can be transferred to the GL via capillary action, enhancing the system's water retention capabilities. The roof in this study, referred to as the Polder Roof, was developed by the Metro-Polder Company. It spans a total drainage area of $32.1m^2$ and includes two subregions with different soil depths. The central region covers $18m^2$ with a soil depth of $20cm$, while the shallower border region covers $14.1m^2$ with a 10 cm depth. Both regions are underlain by a $10cm$ high water retention box

(BL), which supports the upper GL.
As layers one has (starting from bellow): a protective geotextile, that is placed between the system and the upper roof surface; a waterproof membrane, placed above the geotextile and along the border sheets; and a capillary geotextile, surrounding all the BL. Afterwards one has the Perm avoid system that has supports units and capillary columns, and finally, the GL. The integrated monitoring system measures temperature, precipitation, wind speed and water levels in the BL. It took measurements every 10 minutes and transmitted them to an online database.
The analysis was not only performed with the sensors installed in the BGR, in the nearby area there was already installed an advanced weather monitoring system, which included a meteorological weather station and different sensors for rainfall monitoring.
The monitoring system included a Polder roof integrated monitoring system, an external weather monitoring station, and two rain barrels that have water depth sensors and thermometers.
The retention capacity of the GL and the BL was evaluated with respect to the cumulative precipitation in about 170 days during the winter-spring period, that was $232mm$, from which $158mm$ were retained by the system with a distribution of 31% into the GL and 69% into the BL. This means that in the BL there was 3476L of water collected during that period. Another way of contribution was the water that can arise from the runoff and be temporarily stored in the rain barrel. Therefore, it is concluded that the retention efficiency of the system is strongly dependent on the operative management of the SFC system.
As result from the study, it was estimated that the mean retention rate was 77% at the daily scale and about 61% at the event scale. These values come into the range of previous studies that indicate that extensive green roofs can have retention rates between 50% and 80%. Furthermore, the paper emphatically says that these values can be considered as preliminary ones, or better said, the retention rates have to be seen as representative of the minimum retention capacity of the system as it states that it depends on the systems age. Another reason is that in this study there were no operative rules applied, well the control weir was never opened during the monitoring period.
A remarkable thing of this study is that it was the first one on measuring the contribution of the GL and the BL to the retention function of a multilayer green roof, to see how much water can be re-used for other purposes.

3. **Blue green roofs with forecast- based operation to reduce the impact of weather extremes.** Green roofs have been critiqued for their limited

water storage capacity. To address this issue, a solution was introduced by incorporating an additional Blue Layer beneath the traditional Green Layer proposed by T. Busker et al. in [23]. In this study, a model of a blue-green roof system was developed and evaluated using precipitation forecasts to optimize the water retention capacity during extreme rainfall events. A key feature of this system is a valve mechanism that controls the water level within the storage layer, allowing dynamic regulation based on forecasted precipitation. The case study for this investigation was conducted in Amsterdam.
One of the main points highlighted in this paper is the use of a smart forecast-based action system that triggers roof drainage from the blue layer when needed. In fact, the goal is to assess the effectiveness of blue-green roofs in reducing peak discharge by utilizing a smart forecast based on action system that riggers roof drainage from blue layer.
The hydrological model was run with data from 27 weather stations in the Netherlands, so the model can have enough number of extreme events to limit the uncertainty of the hydrological performance indicators.
The daily potential evapotranspiration was forecasted based on the water content in the BL and GL. According to the author, a roof is suitable to be a blue-green roof if it is flat and is larger than $200m^2$. That is because of the economic viability. And to consider a roof flat, one needs to evaluate if more than 60% of its surface has a slope lower than 11°. To filter the extreme events, the researchers assumed that if there was a precipitation higher than $20mm$ in 1 hour, it would be considered as extreme event.
The study concluded that the performance of the Multilayer Blue-Green Roof (MBGR) is least effective during the most extreme rainfall events. Specifically, the system was able to capture only 30% of the precipitation from the most severe event recorded during the testing period. To improve performance, the use of ECMWF ensemble precipitation forecasts was proposed to enable controlled drainage activation prior to such events, allowing the system to optimize its storage capacity in anticipation of incoming rainfall.

4. **Experimental investigation of a multilayer detention roof for stormwater management**

   Purple roofs or detention roofs are the ones that have two additional layers, one detention layer and one water storage layer, this was proposed by M. A. Alim et al. in [24].The research worked with three different types of roofs: one traditional, one green roof and one purple or detention roof. The idea was to evaluate the amount of discharge that each roof let flow after the different storm events. To measure it, two tipping buckets were installed beneath each roof.
   Furthermore, everything gets weighed before being poured into the gardens

in a dry state, except for the plants that are considered to have a constant weight during time. Also, as the gardens are placed over a scale, the wight of the system gets measured every time a precipitation event occurs to monitor the amount of water that falls into the system and how much of it gets to the tipping bucket.
The authors primarily compared the performance of different roof systems for each rainfall event, using a traditional roof as a reference to calculate key hydrological indicators for the other systems. This approach enabled them to assess changes in runoff volume and quantify how it increased or decreased relative to the traditional roof. Additionally, the study references Fleck et al. (2022), who developed a SWMM model to predict peak flow reduction on a green roof in Sydney during a major precipitation event with a 20-year return period (T=20y).

5. **Multi-objective optimization for stormwater management by green-roofs and infiltration trenches to reduce urban flooding in central Delhi.**

   The authors S. Kumar et. Al in [25], use two management and design strategies to control the stormwater runoff. Those are: Best Management Practices (BMPS) and Low Impact Developments (LIDs). It has been said that these techniques save the pre-development hydrologic characteristics by employing decentralized measures on a smaller scale. These practices include green roofs, infiltration trenches, permeable pavements, and bio-retention systems. They also help to improve the water quality and can manage the volume of runoff during peak rainfall. As urbanization reduces the pervious area, it increases the runoff time. Nevertheless, it has to be clarified that the flood reduction of these retention measures depends on the magnitude.
   SWMM is a model used to simulate the streamflow in the urban catchments and compute the urban drainage performance around the globe. In section 3 of the paper, the step by step of the analysis was explained by the authors, where they explain the creation of the SWMM model, the selection of the BMPs and the LIDs, as well as the scenario where they would be implemented. For the selection of the BMPs and the LIDs, there were different scenarios considered depending on the SWMM model and changing some of its characteristics. In this case, there were a lot of possible arrays of BMPs/LIDs. Nevertheless, only three scenarios were considered in this study, but in all of them the goal is the same, know how much the flow can be reduced in each stage.
   To analyze the performance of the models and to select the best positioned BMPs/LIDs and an optimization algorithm and a multi-objective optimization model were used. It does not only consider the technical data, but also the

economical one and the cost of retaliation if such an event occurs.

6. **The hydrological performance of a green roof in Sydney, Australia: A tale of two towers**

   In this paper R. FLeck et al [26] made use of SWMM and DRAINS to perform hydrological models to predict the performance of the green roofs and to identify its ability to manage stormwater runoff and frequency. Another important aspect is that they were used to analyze its performance in complex surface flooding situations where storage or backwater effects occur in overflow routes and surface flows.
   SWMM (Storm Water Management Model) was used to quantify the reduction in stormwater flow rates from the green and conventional roofs into the local stormwater management network based on locally sourced data. On the other hand, the DRAINS was used to predict the fluvial mitigation performance of the green roof. It is one of the most used software to predict design flows and volumes in Australia. What it does is to simulate a storm that has been designed to assist in the Intensity-Frequency-Duration statistic.

Chapter 3

Methodology

In this chapter, the methodology adopted for the simulation of the behavior of a green roof installed in the center of Turin, Piedmont, Italy will be explained. The description goes from the arrangement and the organization of the data to the description of the simulation, all of this performed with the help of the software MATLAB.

The methodology is based on the one adopted by E. Cristiano, F. Lai, R. Deidda and F. Viola in the paper "Management strategies for maximizing the eco hydrological benefits of multi-layer blue-green roofs in Mediterranean urban areas" for the simulation of the behavior of a green roof located in Cagliari, Sardinia, Italy [21].

3.1 Data Calibration

In the previously mentioned paper, the required input data to run the simulation were: Temperature, Rainfall and Potential Evapotranspiration. For the evaluation of the behavior of the Green Roof is important to have a significant sample of data, meaning covering a significant period of time. In this case the data is divided into three periods: Historical, Observed and Future. The data were acquired from ARPA Piemonte [27] for the observations and CMCC (Centro Euro-Mediterraneo sui Cambiamenti Climatici) [28] for both scenarios, historical and future. The goal of this calibration is to compute biases in the mean annual temperature and precipitation estimates, apply corrections, and construct bias-corrected time series. This process is crucial for improving the accuracy of climate model predictions and better understanding regional climate impacts.

Regarding the observed data, there are three measurement stations in Turin that have historical information for Precipitation and Temperature in the city center. They are called: Giardini Reali, Via della Consolata and Buon Pastore. The three

of them are located in the city center, no more than 1.5 kilometers away from each other. Nevertheless, not all measurements were taken in the same station for the whole period of time. So, as they are nearby stations, the data of the three of them was merged and a simple average was performed among the overlapping ones. As a result, a continuous time series of data was obtained, starting from March 1989 until December 2023.

Speaking of both the scenarios, historical and future, they were taken from the CMCC. The future scenario is 65 years long and is based on the IPCC RCP 4.5 scenario. This specific scenario is a moderate one considered to estimate the future projections for both temperature and precipitation in the future scenario, mainly in the period from 2005 to 2100 [29]. This scenarios were part of the Hylander project, that is an open hourly climate projection with a resolution of 2.2 km over Italy. The projections are done with the Regional Climate Model COSMO-CLM and is important to mention that they include a very innovative methodology, well they run regional climate models (CP-RCMs) within grids smaller than $4km$ allowing convection to be solved on the grid without the need of performing a parameterization scheme. All this brings many advantages, such as the sensitivity to climate change of the models and the availability of hourly data. Furthermore, improving the spatial resolution means also to get to know the changes in the surface and let one see the land -atmosphere feedback [29].

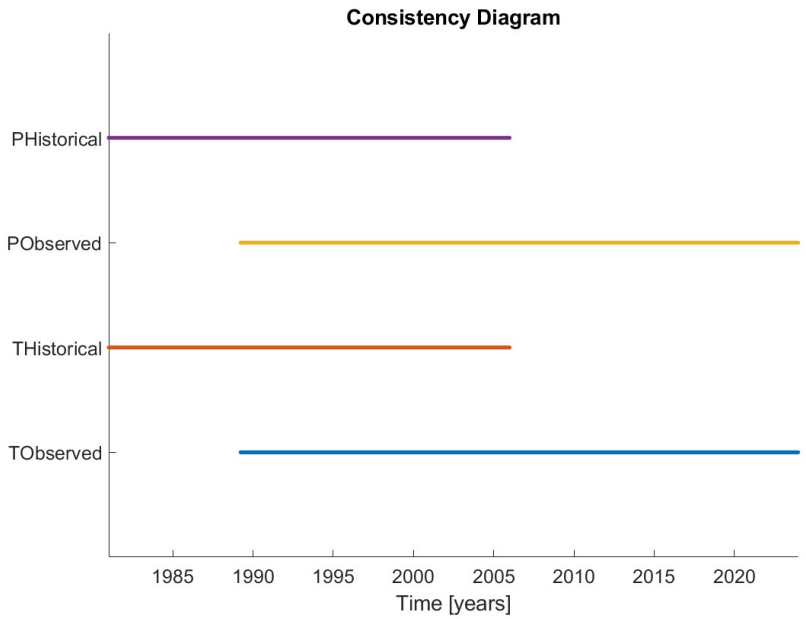

Figure 3.1: Data Consistency Diagram.

Is also important to mention that before starting to analyze the data, one needs to know if there is continuity in the measurements, so a Data Consistency Diagram is to be seen in Figure 3.1. From it, is possible to see that the samples have enough data, apart from a few days in the observed data, that did not have measurements.

For the correction of the data in MATLAB, is important to have the vectors of the observed and historical data of the exact same length. As it is possible to see in Figure 3.1, there is a constant period of time, where the data overlap. That is why, the vectors for the correction process were trimmed starting from "01/01/1990" until "31/12/2005". Also, the correction process is divided into two, one part is for the calculation of the Temperature bias and the other part is for the calculation of the precipitation bias.

3.1.1 Temperature

Before starting with the correction, is important to see how the historical and observed data behave. In figure one can see that there is an evident difference, so a bias calculation is possible to correct the future scenarios.

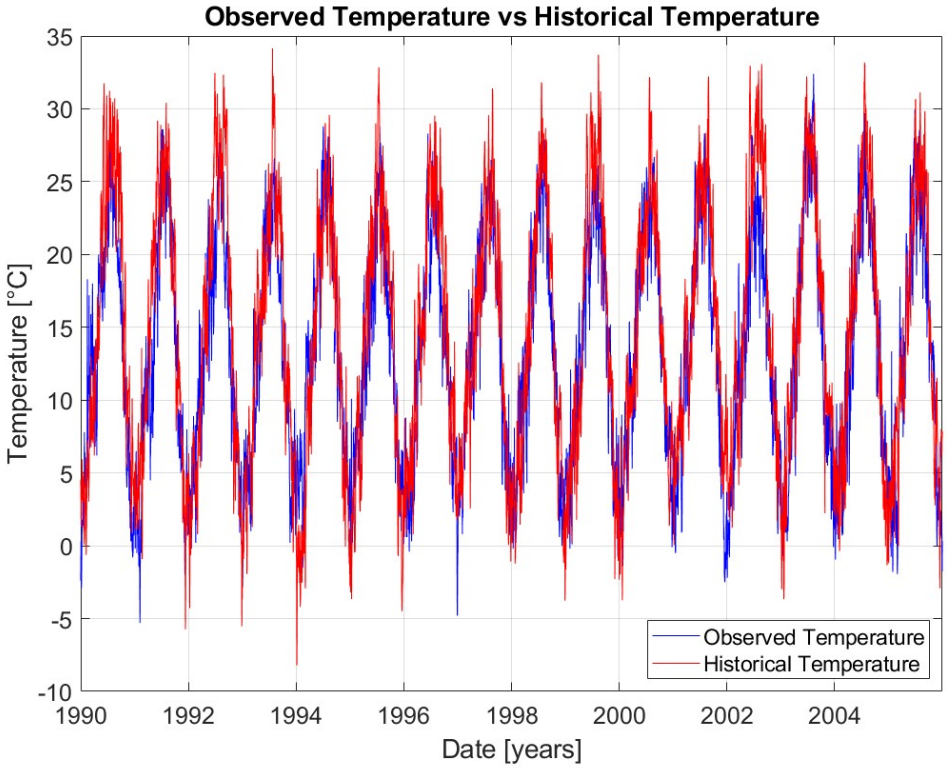

Figure 3.2: Observed vs. Historical Temperature.

One wants to calculate the mean monthly value for each month considering all years. To do so, one has to calculate the monthly mean value of the temperature throughout all the years. At the end, one will obtain 12 values, one for each month of the year.

$$\overline{T}(m) = \frac{1}{N} \sum_{y=1}^{N} T(y, m) \tag{3.1}$$

The same equation is used for both historical and observed data, so the process needs to be performed two times, one for each dataset. Where $\overline{T}(m)$ is the mean temperature for the month m, N is the number of years in the dataset and $T(y, m)$ is the temperature for year y and month m.

After having calculated both observed and historical mean temperatures, each of them containing 12 values, the temperature bias can be calculated.

$$\Delta T(m) = \overline{T}_{\text{obs}}(m) - \overline{T}_{\text{hist}}(m) \tag{3.2}$$

As a result, one gets the Figure 3.3 with the values of the temperature biases that were then applied to the scenario values, so they get corrected.

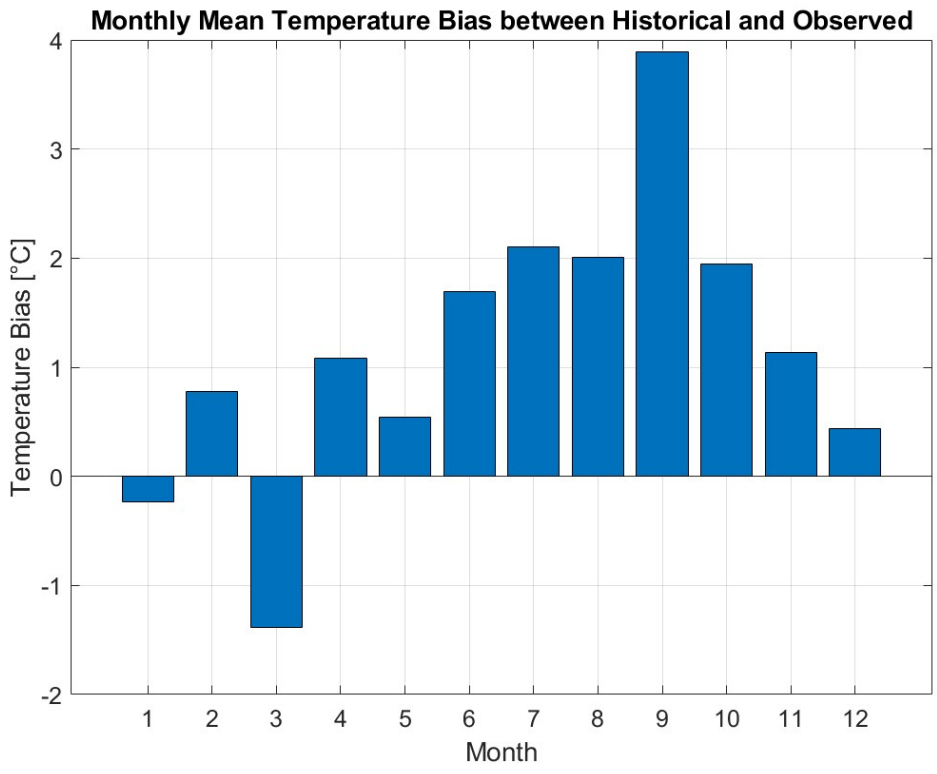

Figure 3.3: Temperature Bias.

With the calculated biases one can perform the correction for the whole future scenario data set or for the required period of time that one needs for an specific analysis, as can be seen in equation 3.3. In this case, the correction will be performed for the whole future scenario dataset, so the simulation of the behavior of the green roof can be seen in a long period of time, which is illustrated in Figure 3.4.

$$T_{\text{future corrected}}(y, m) = T_{\text{future}}(y, m) + \Delta T(m) \tag{3.3}$$

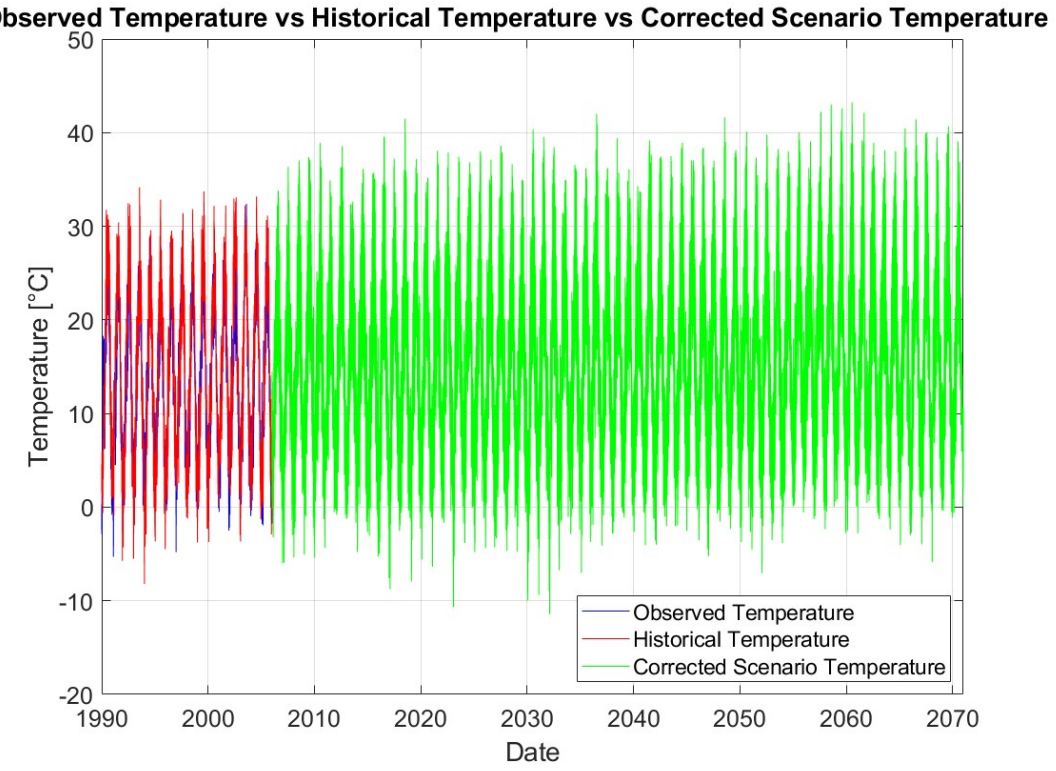

Figure 3.4: Corrected Temperature.

3.1.2 Precipitation

For precipitation data, the analysis was slightly more complex due to the inherent variability and seasonality of precipitation. Firstly, a comparison between the ground-based observational data from ARPA Piemonte and the historical data was performed, focusing on monthly aggregated values to capture seasonal variations.

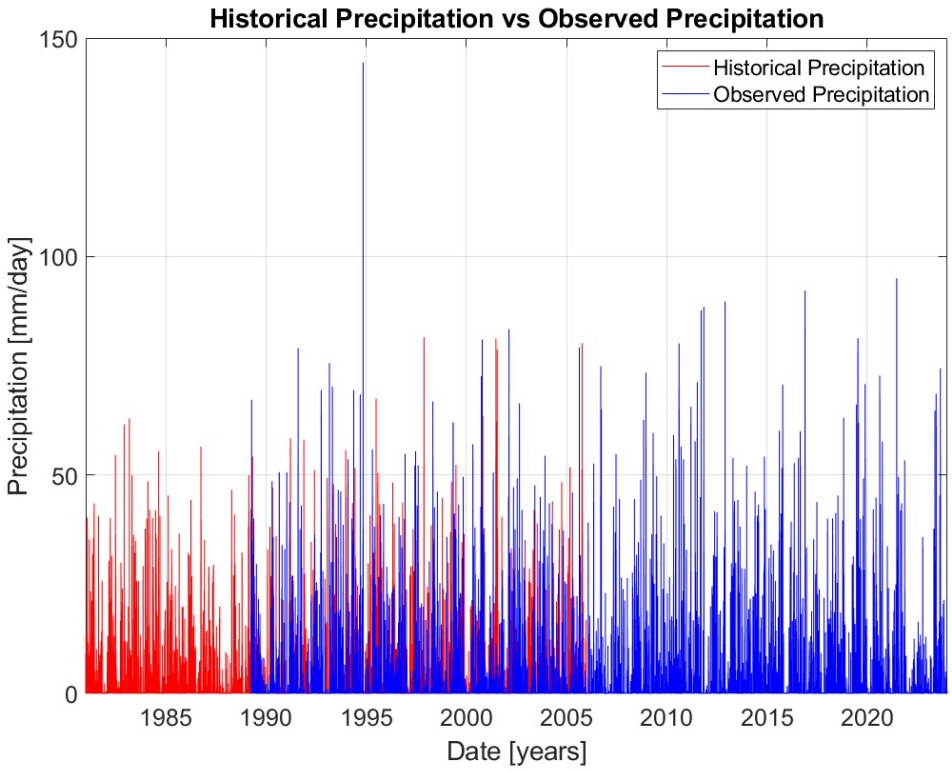

Figure 3.5: Observed vs. Historical Precipitation.

In Figure 3.5 is possible to see that both historical and observed data have a similar behavior, considering that the one with the higher peaks is the observed one.

The process for the assessment of the mean monthly precipitation is performed in the same way as the temperature, calculating the monthly mean value of precipitation throughout all the dataset years.

$$\overline{P}(m) = \frac{1}{N} \sum_{y=1}^{N} P(y, m) \tag{3.4}$$

Where $\overline{P}(m)$ is the mean precipitation for the month m, N is the number of years in the dataset and $P(y, m)$ is the precipitation for year y and month m. Already having the two vectors with the 12 mean values for the historical and the observed data, one can proceed to calculate the bias. In this case, the process is similar to the one with the temperature but instead of making a subtraction, a ratio between observed and historical is performed.

$$Ratio(m) = \frac{\overline{P}_{\text{obs}}(m)}{\overline{P}_{\text{hist}}(m)} \tag{3.5}$$

Where $\overline{P}_{\text{obs}}(m)$ is the observed mean precipitation for month m and $\overline{P}_{\text{hist}}(m)$ is the historical mean precipitation for month m. After having calculated the ratio, one continues to perform the multiplicative correction of the future scenario data of precipitation as seen in Figure 3.6.

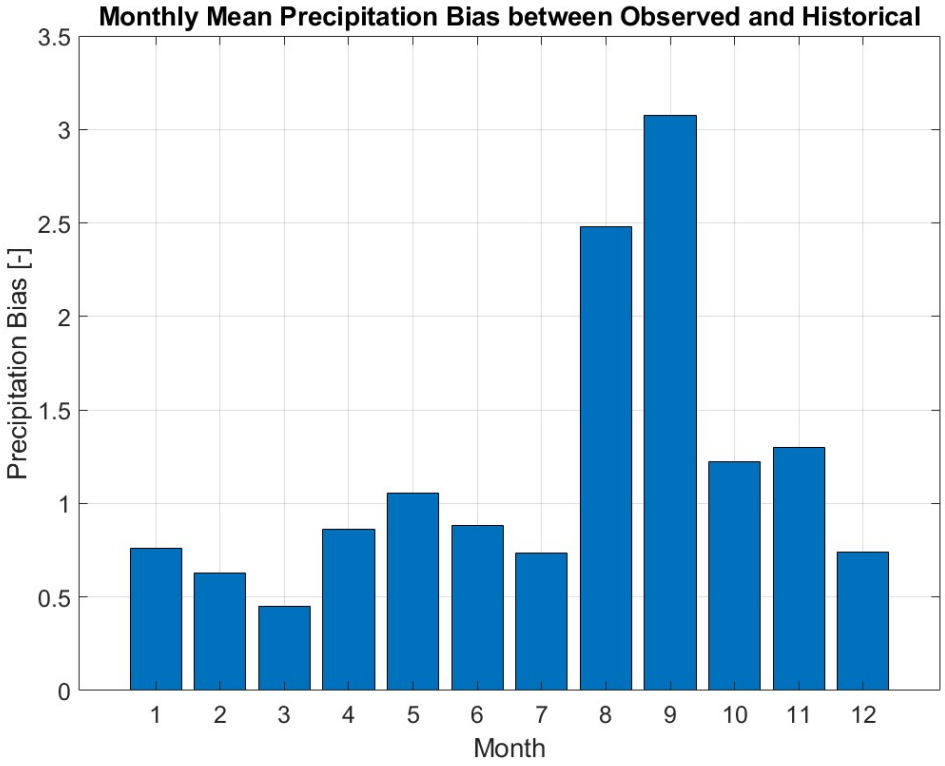

Figure 3.6: Precipitation Bias.

$$P_{\text{future corrected}}(y, m) = P_{\text{future}}(y, m) \times Ratio(m) \tag{3.6}$$

Where $P_{\text{future}}(y, m)$ is the future scenario precipitation for year y and month m and $Ratio(m)$ refers to the one calculated in Equation 3.5. The results of the correction can be seen in the Figure 3.7.

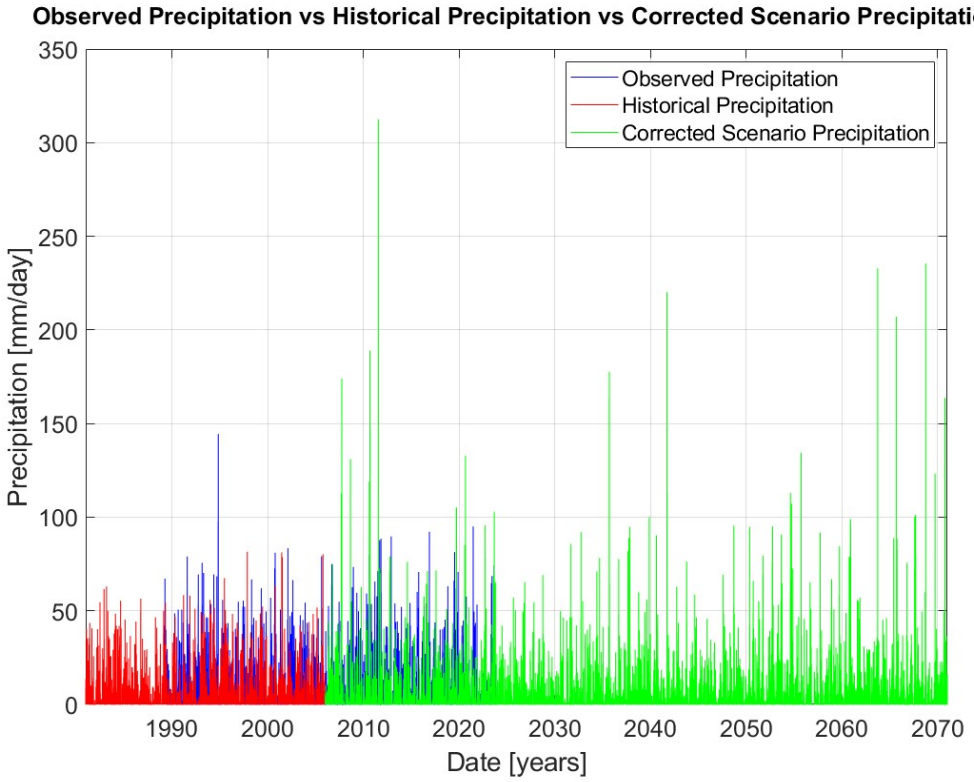

Figure 3.7: Corrected Precipitation.

3.2 Potential Evapotranspiration Calculation

Evapotranspiration is a key element of the hydro-logical process. it combines the processes of transpiration and evaporation of water. The first one refers to the evaporation of water from the plants, and the second one refers to the same process but related to the soil. In the water cycle it helps to know how much water is returned to the atmosphere through vapor and does not percolate to the soil. More precisely, potential evapotranspiration (PET) represents the maximum amount of water that could evaporate and transpire from a uniformly vegetated surface, such as a fully irrigated, short green crop that completely shades the ground.[30]

In this analysis the data is handled in both hourly and daily scale. The potential evapotranspiration (ET_0 or PET) is calculated on a monthly scale according to the Thornthwaite method. Is worth noting that for temperatures higher than 26.5 °C, an extra correction has to be performed according to the Willmot et al (1985). [31]

$$PET = \begin{cases} 0 & T \\ 16\left(\frac{10T}{I}\right) & 0°C \leq T < 25.5°C \\ -425.85 + 32.24T - 0.43T^2 & T \geq 26.5°C \end{cases} \tag{3.7}$$

Where T is the mean monthly temperature and a is an exponent that depends on a and the thermal index I as it can be seen in Equations 3.8 and 3.9.

$$a = 6.75 \times 10^{-7} I^3 - 7.71 \times 10^{-5} I^2 + 1.7912 \times 10^{-2} I + 0.49239 \tag{3.8}$$

$$I = \sum_{n=1}^{12} (0.2T)^{1.514} \tag{3.9}$$

In the case of the daily PET calculation, an adjustment in the equation was performed [32]. It consists on multiplying the standard monthly potential evapotranspiration by a correction factor C.

$$C = \frac{N}{360} \tag{3.10}$$

Where C is the correction factor and N is the photo-period (in hours) for a given day.

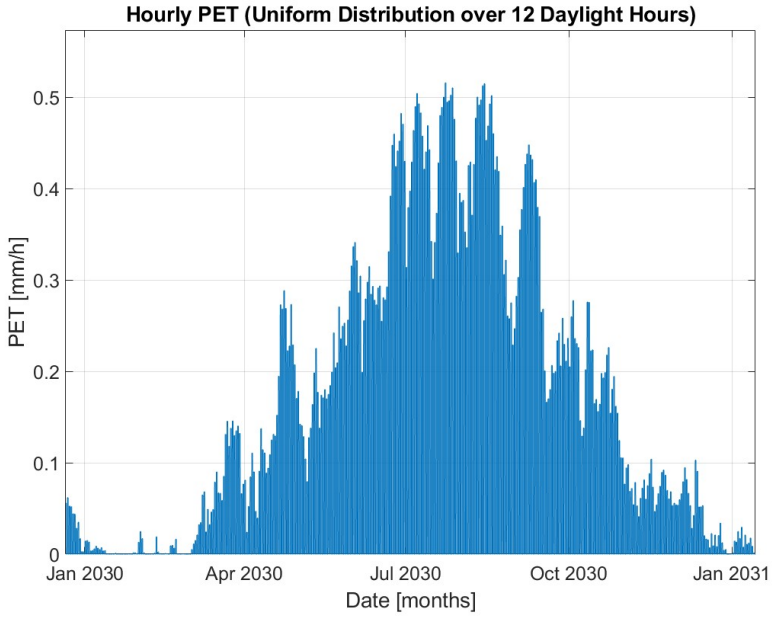

Figure 3.8: Hourly scale PET over one year.

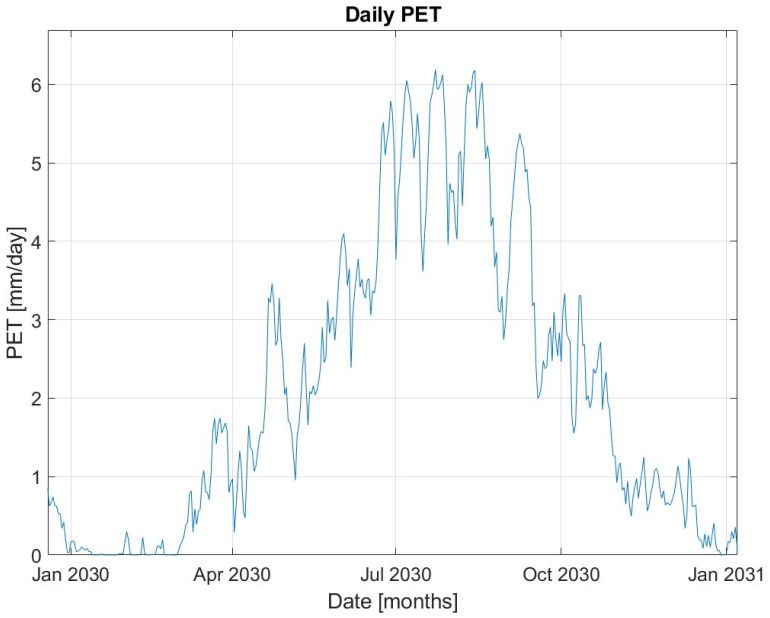

Figure 3.9: Daily scale PET over one year.

After having calculated the values of daily PET, the conversion into hours was performed in a simple way. As the values need to be hourly, one must divide the daily evapotranspiration into the amount of sunlight hours that each day has. Nevertheless, knowing that the daily sunlight changes throughout the whole year, an approximation of 12 hours a day was made. That is why, for seeks of simplicity, the value of the PET was divided by 12 and assigned for the period of time between 6 in the morning and 18 in the afternoon and leaving the rest of the hours of the day with a 0 as value for PET. In Figures 3.8 and 3.9 is possible to see an example of the PET calculation in both hourly and daily scale respectively. From them is possible to see that the behaviour is the same, the order of magnitude of the y axis is the main change.

3.3 Model Description

The behavior of the green roof is analyzed according to the Ecohydrological Streamflow Model (EHSM) proposed by f. Viola, D. Pumbo and L.V. Noto in [33]. The EHSM is a conceptual lumped model designed to simulate daily streamflow in natural river basins. Where a lumped model in hydrology means that it is treated as a single unit, without dividing it into smaller spatial units or sections in the horizontal plane, intending without considering spatial variability [34]. Nevertheless, the model has been adjusted to simulate the hydraulic behavior of a Green Roof by

changing its parameters according to the work presented by E. Cristiano, F. Lai, R. Deidda and F. Viola in [21]. The input variables for the model are both daily and hourly temperature, precipitation and also potential evapotranspiration.

On the other hand, parameters such as the active soil depth (nZr) that refers to the height available for water storage (calculated as the multiplication of the porosity and the soil depth) and the crop coefficient (K_c) are fixed parameters for the initial simulation. Then in later simulations, the parameters are varied to analyze the model's sensitivity and response to changes in its value.Other parameters as the wilting point and the field capacity depend on the type of soil that is being used and are estimated according to literature in this case according to F. Laio, A. Porporato, L.Ridolfi and I. Rodriguez-Iturbe in [35]. The selected soil is classified as loamy sand, which indicates the values for the wilting point, the field capacity and the porosity that helps to get the value of the active soil depth.

In this case the selected Green Roof features a surface area of 16 m2, with a multilayered structure comprising a total thickness of $19cm$, of which $9.5cm$ is a loamy soil substrate. With a soil porosity $nof 0.43$, the active soil depth (nZ_r) is approximately 40 mm. Furthermore, some values were selected from literature for that type of soil, which are 0.52 for the field capacity (s_t) and 0.08 for the wilting point (s_w)[35].

It is worth mentioning that the specific weight of the loamy sand is $15\frac{kN}{m^3}$ [36]. Also, under saturation and with a porosity of 0.43 one arrives to a saturated specific weight of $19.3\frac{kN}{m^3}$. And for this Green Roof that has cases with two different thicknesses, the weight of the substrate layer per square meter can be seen in Table 3.1.

Case	Dry Unit Weight $[\frac{kN}{m^2}]$	Saturated Unit Weight $[\frac{kN}{m^2}]$
Cases 1,2 and 3	1.43	1.84
Case 4	2.85	3.67

Table 3.1: Unit weight of the substrate layer in dry and saturated conditions

In the code, the model represents basically the hydrological balance of a standard green roof. It aims to show the response of the roof to a precipitation event, while analyzing what comes in and exits the system in form of simulated discharge. Firstly, the rain falls in the soil layer and starts infiltrating into the soil layer. Is important to notice that the soil layer is designed to be kept at least at the wilting point (s_w), where it is guaranteed that the vegetation of the system is able to survive with the minimum of the resources. Knowing that, the precipitation that arrives to this layer starts to filter into the soil and it, in relationship with the soil moisture of the terrain, starts generating a Leakage that percolates the terrain and exits the system through an output. In saturation case, when the soil moisture of

the terrain is equal to 1 (and meaning that all the voids of the soil are filled with water) the presence of Runoff appears. [21]

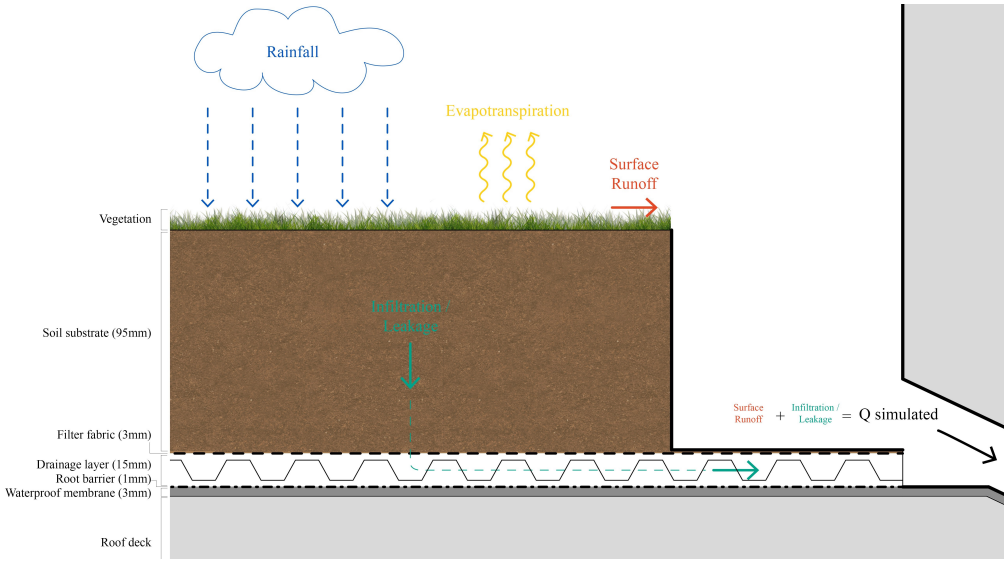

Figure 3.10: Hydrological Balance of the Green Roof.

Is important to mention that depending on the type of vegetation, the canopy interception has to be considered and therefore the rainfall that passes through the vegetation gets calculates, as illustrated in Equation 3.11.

$$Throughrainfall = Rainfall - Interception \tag{3.11}$$

In the model, the behavior of the soil is influenced by its porosity n and its depth Z_r, which results in the active soil depth nZ_r. Nevertheless, the variation of the water content in the soil layer is dynamic and depends on different variables as shown in Equation 3.12. [33]

$$\Delta s = \frac{1}{nZ_r}(R - ET - L - Ru) \tag{3.12}$$

Where Δs is the change in the water content in the soil layer of the green roof and R refers to the rainfall. In this project, the water losses are considered separately, where ET means the actual evapotranspiration, L is the leakage of water due to deep percolation in the system and Ru refers to the excess saturation surface runoff. The latter refers to the runoff only when the soil gets saturated [33]. Nevertheless, is important to clarify that for the results analysis, the water losses are going to be considered as one, meaning both the leakage and the runoff values.

$$ET = \begin{cases} 0 & 0 < s < s_0 \\ E_w + \frac{(E_{max} - E_w) \times (s - s_0)}{(s_t - s_0)} & s_0 < s < s_t \\ E_{max} & s_t < s < 1 \end{cases} \tag{3.13}$$

$$E_{max} = PET \times K_c \tag{3.14}$$

$$L = \begin{cases} 0 & 0 < s < s_t \\ (s - s_t) \times nZ_r & s_t < s < 1 \end{cases} \tag{3.15}$$

Where s_0 is the soil water content at the wilting point, s_t is the field capacity, K_c is the crop coefficient and E_w is the evaporation at the wilting point.

$$Ru = \begin{cases} 0 & 0 < s < 1 \\ (s - 1) \times nZ_r & 1 < s \end{cases} \tag{3.16}$$

In the drainage/reservoir layer (as can be seen in Figure), where it is assumed that there is no accumulation of resources and all the water is discharged immediately, the discharge is considered equal to the leakage. Moreover, when there is saturation of the soil, the excess saturation surface runoff is summed to the leakage.

$$Q_{simulated} = \begin{cases} L & s < 1 \\ L + K_{sup} \times (H_{sup}(i - 1) + R & 1 < s \end{cases} \tag{3.17}$$

Where K_{sup} is the residence time (in this case considered equal to one), H_{sup} is the water height in the surface layer, R is the excess saturation surface runoff and i is the day for which the calculation is being performed.

Is important to mention that after the calculation of the parameters, the duration curves have to be plotted to see the behaviour of the green roof. The calculated and plotted graphs are the: Flow Duration Curve (FDC), Evapotranspiration Duration Curve (EDC) and the total Runoff Duration Curve (RDC).

Chapter 4

Results

In this chapter, the response of the system is evaluated for the different scenarios, both Historical and Future. To do so, different variations in the parameters of the Green Roof are applied. This variations are related to the type of vegetation that the roof is going to have, namely the changes in the crop coefficient K_c and in one case, also the duplication of the active soil depth nZ_r. Regarding the values of K_c is worth mentioning that it corresponds to the stabilized value and not to the one in the early stages. The changes applied to the model are shown in Table 4.1. Basically, the aim of the parameters variation is to see the response of the Green Roof to the same meteorological conditions with different settings, so one can select the best alternative for the vegetation. It is important to mention that the data are treated in both hourly and daily scale, depending on the analyzed parameter.

Case	K_c	$nZ_r[mm]$	**Type of vegetation**
1	0.5	40	Sparse succulent
2	0.85	40	Dense succulent
3	1	40	Herbaceous
4	1	80	Herbaceous

Table 4.1: Different cases for the modelling.

Furthermore, it is worth highlighting that the results are mainly focused on the variables of the hydrological balance, mainly the precipitation (or rainfall), the Evapotranspiration, the Leakage and the superficial runoff, where the last two exit the Green Roof as the simulated discharge. All this, as described in the Figure 3.10 of the chapter 3.

4.1 Historical Simulation

Figure 4.1 presents the time series of the precipitation for the historical scenario that goes from 1981 until 2006 at an hourly scale. It is worth mentioning that the data used in this chapter was already corrected as described in section 3.1.

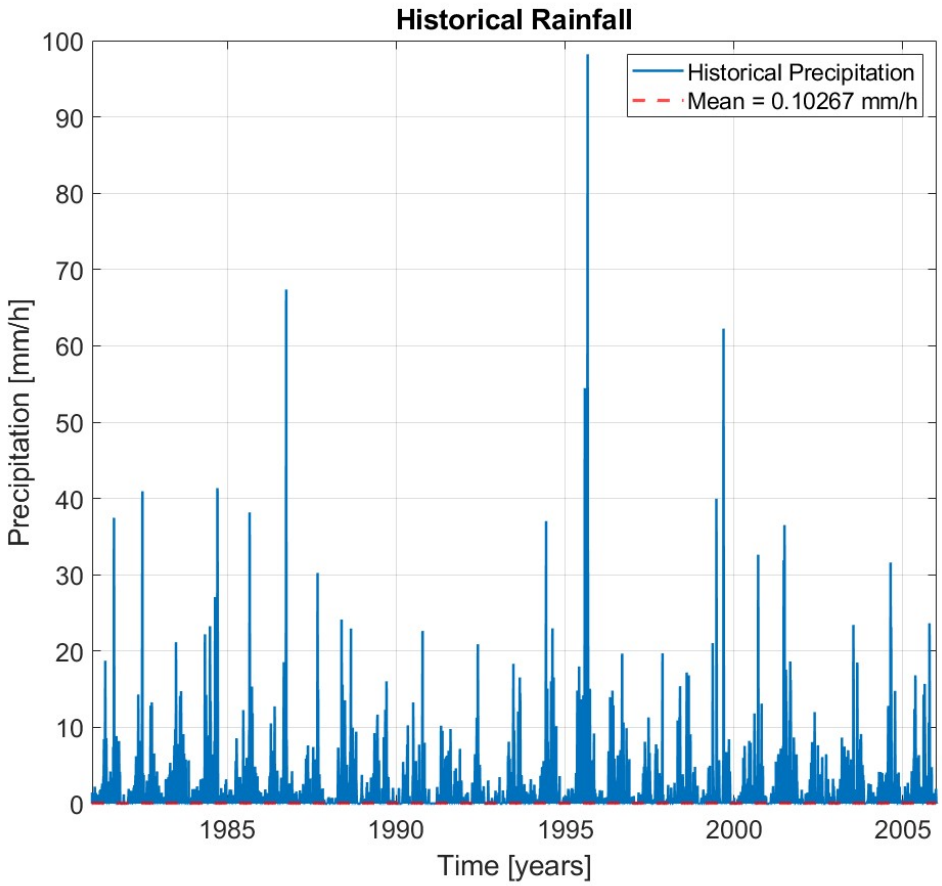

Figure 4.1: Hourly scale time series of precipitation for the historical period.

From Figure 4.1 is possible to see that the mean hourly value of precipitation corresponds to $0.103\frac{mm}{h}$ and that the peaks normally oscillate between 10 and $40\frac{mm}{h}$, except for three values that present precipitations over the $60\frac{mm}{h}$, and reaching a maximum peak of $98\frac{mm}{h}$. Comparing the value of the peaks with the mean one, is possible to see that the value of the peaks is significantly high and shows the events of big intensity. Furthermore, the time series of precipitation allows one to infer that extreme events may not follow strict seasonal trends, due to the large peaks occurring sporadically.

4.1.1 Evapotranspiration

Different from the Precipitation time series, in terms of Evapotranspiration it is possible to see the seasonality and the increase on the evapotranspiration values during the times of the year with more sun-light hours and also higher temperature values. This periodic pattern is typical of seasonal variations, where evapotranspiration peaks are regularly at specific intervals, in this case up to $0.23\frac{mm}{h}$. In Figure 4.2 is possible to see that the mean value is equal to $0.028\frac{mm}{h}$, showing that most of the data fluctuate above and below this average, where the higher values correspond to the warmer periods of temperature on a year.

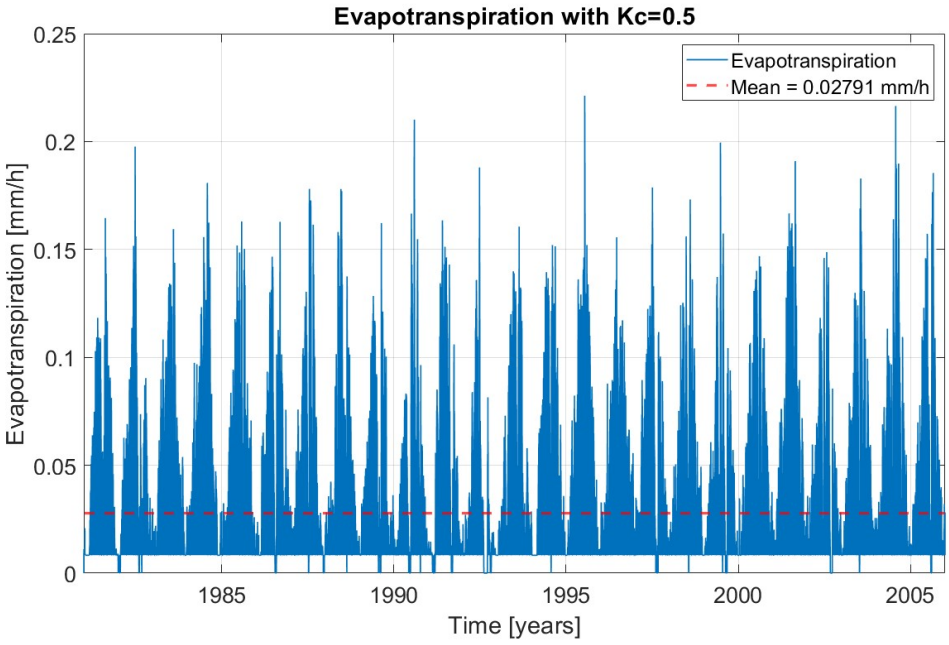

Figure 4.2: Hourly scale time series of evapotranspiration for the historical scenario with $K_c = 0.5$.

Historical Evapotranspiration Duration Curve

The following curve, shows the percentage of time where a certain value of evapotranspiration (presented in the y-axis) was equaled or exceeded in the historical period.

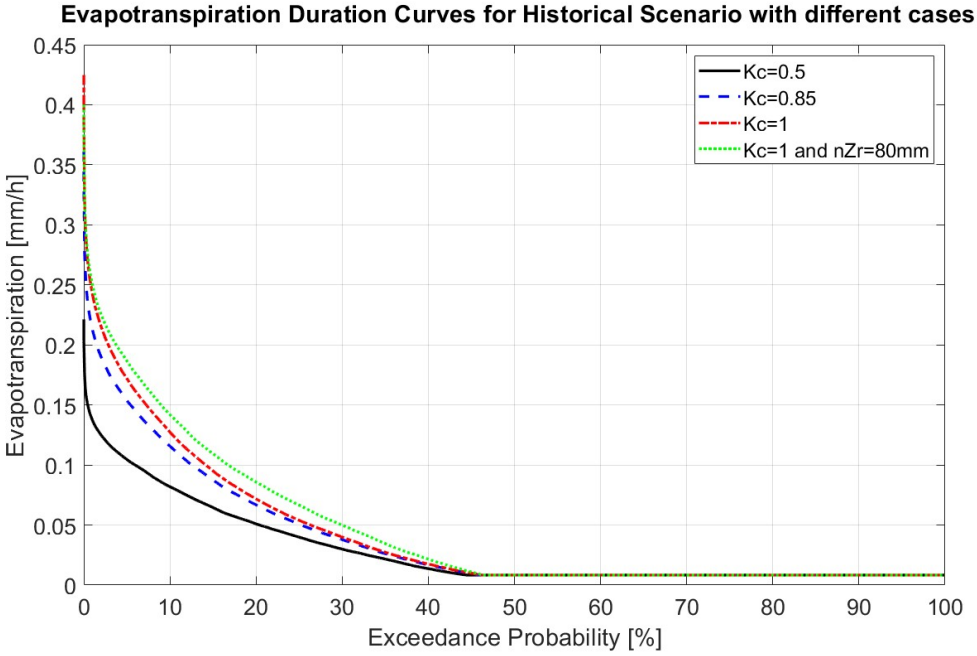

Figure 4.3: Evapotranspiration Duration Curve for the historical scenario with the four different cases.

As observed in Figure 4.3, an increase in the K_c value corresponds to a rise in the maximum evapotranspiration rate, spatially in the rare events (the ones corresponding to the low exceedance probability). Also, a general increment in the evapotranspiration values can be appreciated as the K_c increases. Interesting is that after the 45% of the exceedance probability the evapotranspiration value gets to its minimum, corresponding to the value of evapotranspiration at the permanent wilting point, which means than more than 50% of the time the evapotranspiration rates are minimal.

4.1.2 Simulated Discharge (Q_s)

The simulated discharge values are accounted for the hours on which there was a precipitation event big enough to create either Leakage in form of percolation or superficial runoff in the system. These days can be seen in the Figure 4.4, where the time-series of the discharge with a $K_c = 0.5$ can be appreciated.

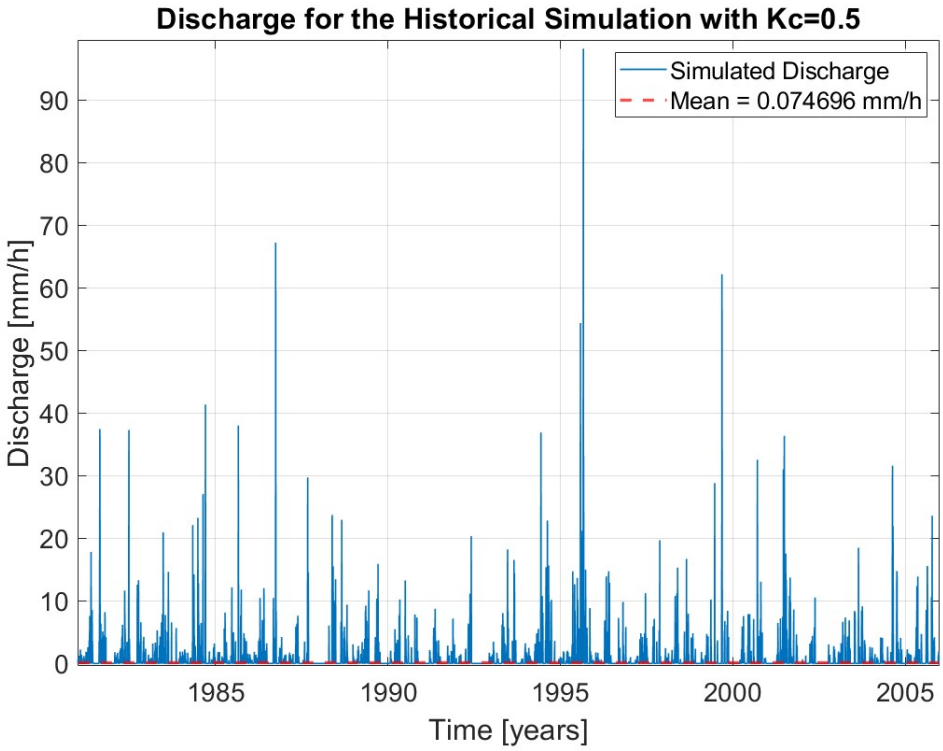

Figure 4.4: Hourly scale time series of discharge for the historical scenario with $K_c = 0.5$.

One can see that there are some rear peaks that are higher than $40\frac{mm}{h}$, while the most of the discharge peaks that there are in the system oscillate until the $10\frac{mm}{h}$. Nevertheless, it is possible to see that the discharge amount is significantly smaller than any of the peak values, which can be seen in the values of the mean discharges. Moreover, in the Table 4.2 is possible to see the differences in the discharge mean across the cases.

Case	$Q_s[\frac{mm}{h}]$
1	0.075
2	0.067
3	0.064
4	0.057

Table 4.2: Mean discharge (Q_s) for the Historical Scenario.

As the K_c of the vegetation gets increased, the retention capacity of the system increases as well, resulting into a reduction of the mean simulated discharge. The

difference in terms of mean discharge between case 1 and case 3 is of 15%. And when the herbaceous case gets a higher soil depth, the reduction in terms of mean discharge is of 24%.

Case	Annual Averages			Other Metrics		
	Precip $[\frac{mm}{y}]$	ET $[\frac{mm}{y}]$	$Q_s[\frac{mm}{y}]$	Days with $Qs = 0[\frac{d}{y}]$	Hours with $Qs = 0[\frac{d}{y}]$	$\Psi[-]$
1	900	245	655	297	8170	0.73
2	900	314	586	307	8262	0.65
3	900	337	563	310	8290	0.63
4	900	396	503	316	8337	0.56

Table 4.3: Comparison of Cases for Precipitation, ET, Qs, and Number of Days/Hours with $Q_s = 0$ in the Historical Scenario.

When analyzing the historical simulation, Table 4.3 illustrates the behavior of three parameters of the hydrological balance of the Green Roof on a yearly mean in the first part of the table. Here, one can see, on a bigger scale, what has been stated before about the increase on the simulated discharge among the different cases. Conversely, when analyzing the evapotranspiration (ET) results is possible to see that as the K_c increases, there is also more evapotranspiration. Changing from case 1 to case 3 shows an increment of almost 38%.

Historical Flow Accumulation Curve

The aim of this accumulation curve is to display the behavior of the green roof in terms of flow attenuation. It also presents the four different simulation cases, with the cumulative precipitation volume included as a reference to see how their behaviour is related. This plot helps to understand the consistency of the model in terms of the flow attenuation.

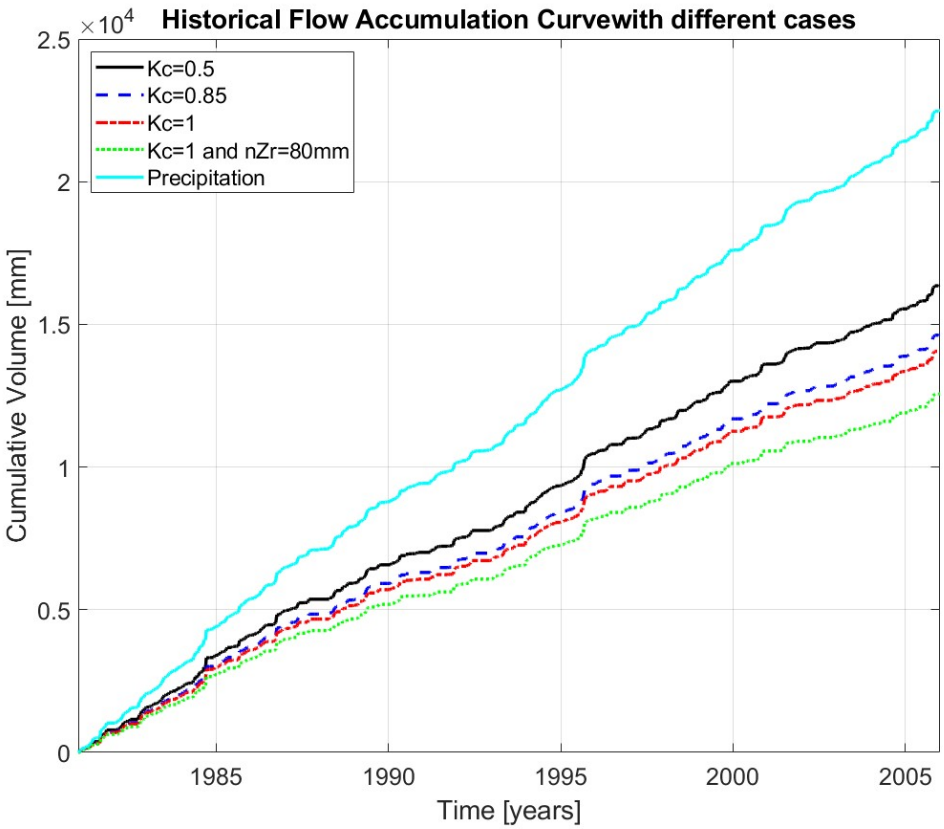

Figure 4.5: Comparison historical FAC for precipitation and simulated discharge for the different cases.

In the Figure 4.5 it is interesting to see that almost in the middle of the historical period, there is a sudden increment in the cumulative volume. This significant increment is due to the biggest precipitation event that happened on that day and that is the reason for such a stiff slope during that period. On the other hand, in general terms, the behavior of the cumulative volume for the simulated discharge in the different cases show a flatter slope, meaning periods of reduced stream flow. In the parts where there is a sudden increment or a considerable increment in the slope, means that there was a higher flow rate. Also, it is worth mentioning that the difference between the cumulative precipitation and the discharge is the amount of water that gets evapotranspirated in the system.

4.2 Future Simulation

The aim of this simulation is to evaluate the performance of the Green Roof in the future to mitigate the impact of the extreme precipitation events that may happen.

The data are analyzed is for a period of 65 years, starting from 2006 and going until 2070 [28]. In the model for the future scenario, the data was split into three different periods. The first one is the Near Future scenario that goes from 2006 to 2027, the second one is the Mid Future scenario starting from 2028 until 2049 and the last one is the Far Future scenario from 2050 until 2070. In Figure 4.6 it is possible to appreciate the predicted precipitation with the data already divided in the three different periods previously mentioned.

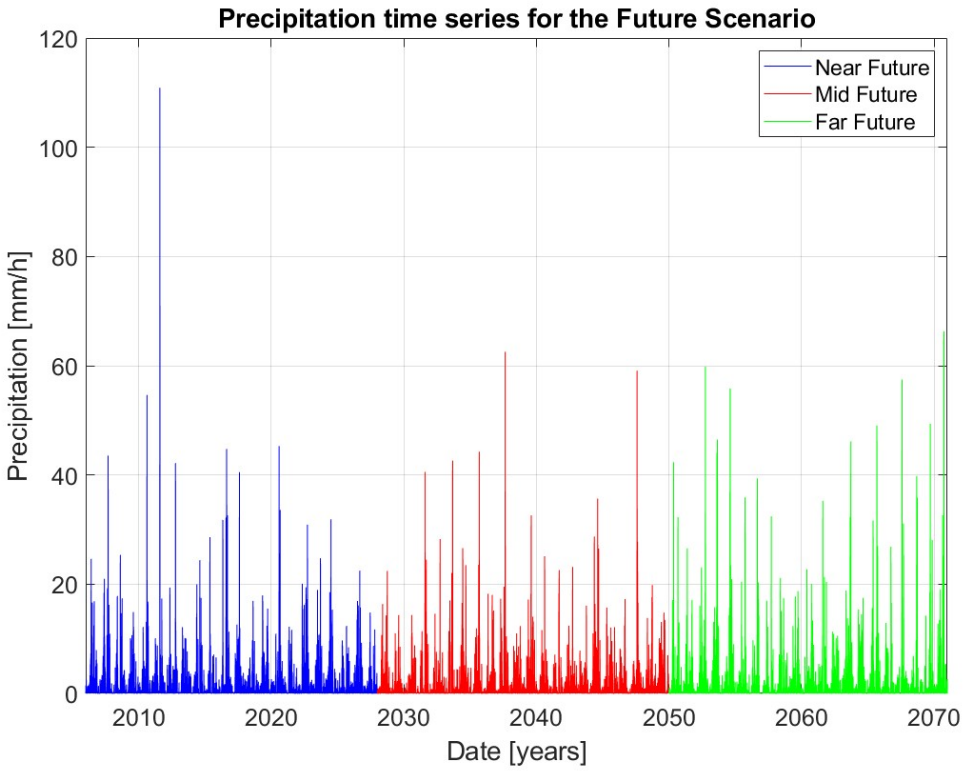

Figure 4.6: Hourly scale time series of precipitation for the future periods.

4.2.1 Evapotranspiration

Evapotranspiration is a key element in the horological balance of the Green Roof, because it represents the actual amount of water that is removed from the system's soil and vegetation in form of both evaporation and transpiration. In the following time series it is possible to see the hourly variation of the evapotranspiration for the whole future scenario.

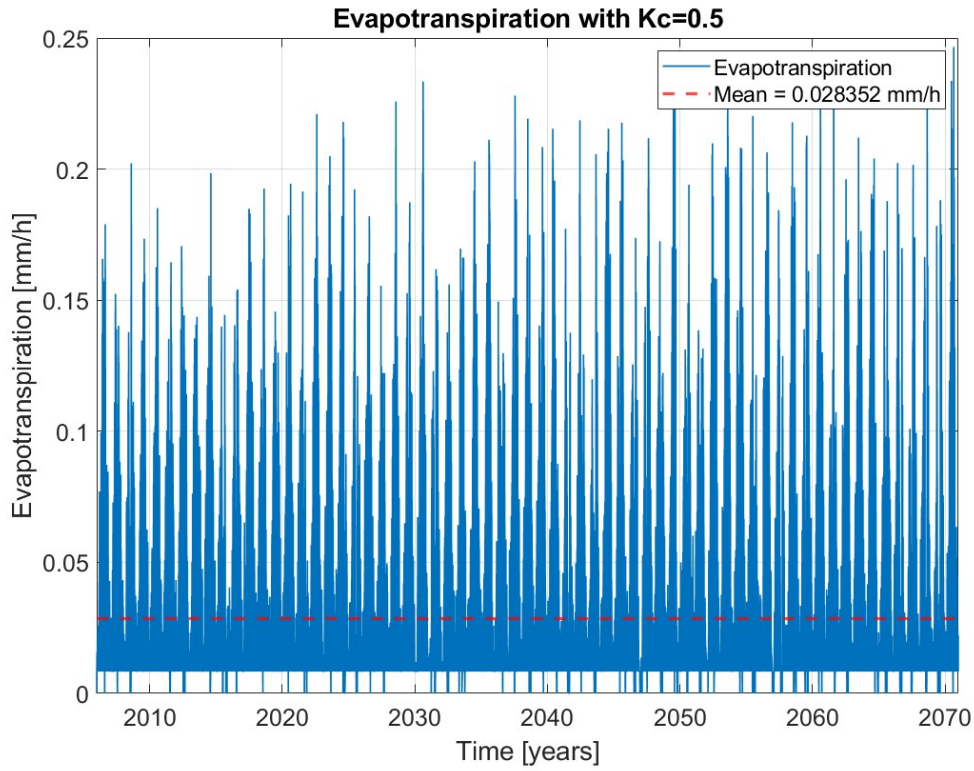

Figure 4.7: Hourly scale time series of evapotranspiraton for the future scenario with $K_C = 0.5$.

From Figure 4.7, it is evident that the hourly evapotranspiration values vary between the minimum value corresponding to the evapotranspiration at the wilting point of $0.0083\frac{mm}{h}$ and a maximum near $0.25\frac{mm}{h}$. It is important to highlight that this minimum value depends on the soil moisture, more exactly the value of the soil moisture at the permanent wilting point (s_w). However, these extreme values occur not so often, and the majority of the data falls within a more typical range. This can be observed in the darker blue regions of the figure, which correspond to values between $0.0083\frac{mm}{h}$ and $0.05\frac{mm}{h}$. The mean evapotranspiration rate over the entire future period is calculated to be $0.028\frac{mm}{h}$, highlighting the predominance of lower rates of evapotranspiration across the analyzed time frame.

Evapotranspiration Duration Curve (EDC)

As the one in the historical scenario, this curve is a cumulative frequency curve that indicates the percentage of the time when a certain value of evapotranspiration was equal or exceeded. It is also important to mention that the Figure 4.8 has the curves for all the four analyzed cases.

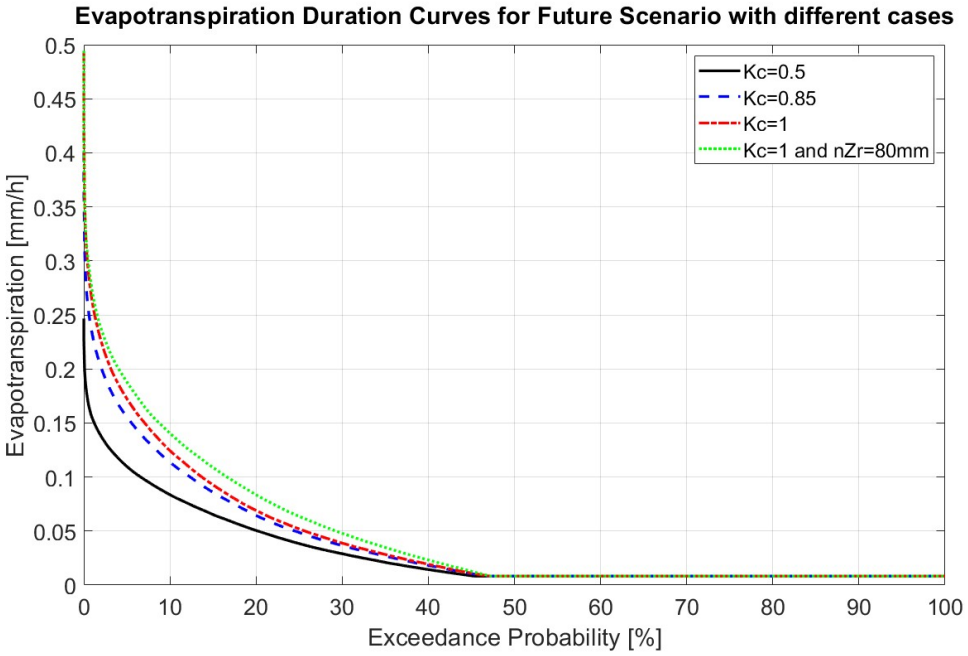

Figure 4.8: EDC for the whole future scenario with the four cases.

In Figure 4.8 shows maximum values of around $0.5\frac{mm}{h}$ for both case 3 and 4, which corresponds to very low exceedance probability and indicates that such values appear on very few occasions along the whole analyzed period. As the exceedance probability starts to increase, the evapotranspiration values start to become smaller. Until the part when the 20% of exceedance propability it is possible to see the difference in the curves for each of the four cases. As the K_c is smaller, less evapotranspiration occurs in the system. The flat behaviour that starts from the 50% and goes on, tells that lower evapotranspiration rates occur for slightly more than half of the time. This because, as it is on an hourly scale, and from the assumption previously mentioned, the daylight period is considered as 12 hours a day for a matter of simplification. Additionally, one can see that the graph does not arrive to zero, what corresponds to the evapotranspiration at the wilting point.

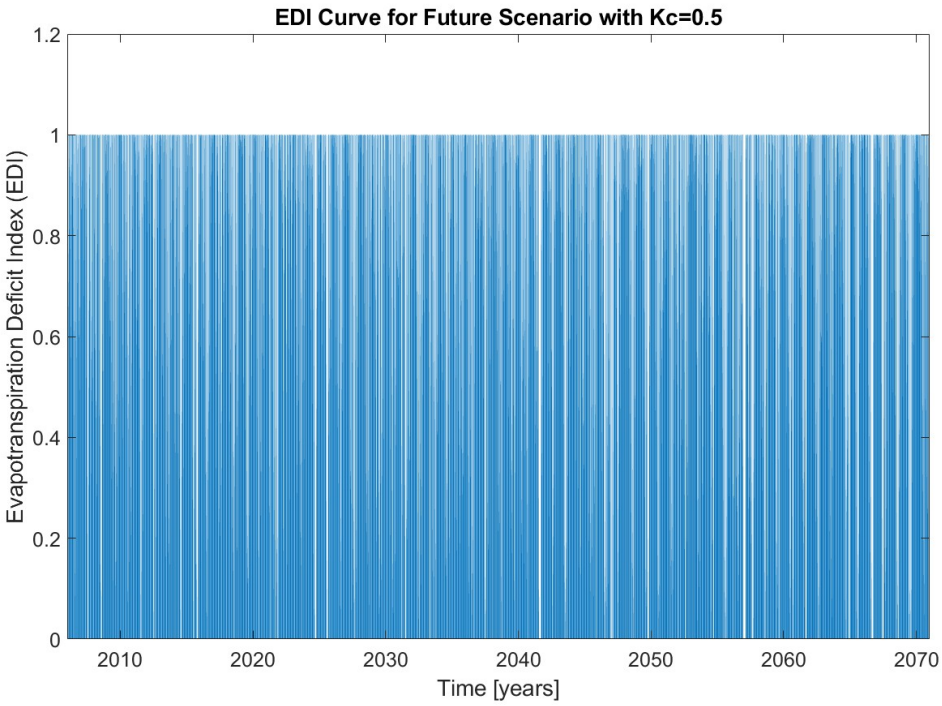

Figure 4.9: Evapotranspiraton Deficit Index (EDI) over the whole future scenario.

In Figure 4.9 is not very easy to differentiate the changes in the values of the index. Mainly, it is because of the hourly scale, where everyday of the total future scenario has both hours with changes in the evapotranspiration rate during the day and zero evapotranspiration during the night, what results in such a graphical representation. Later, in the section 4.2.1 one can appreciate the differences between day and night in a better way.

Evapotranspiration for an example year (2030-2031)

To appreciate better the behaviour of the system and see the changes graphically from the different curves, an example year was selected in the mid Future Scenario. During the example year period is possible to see an example month, so the hourly changes in the evapotranspiration can be appreciated.

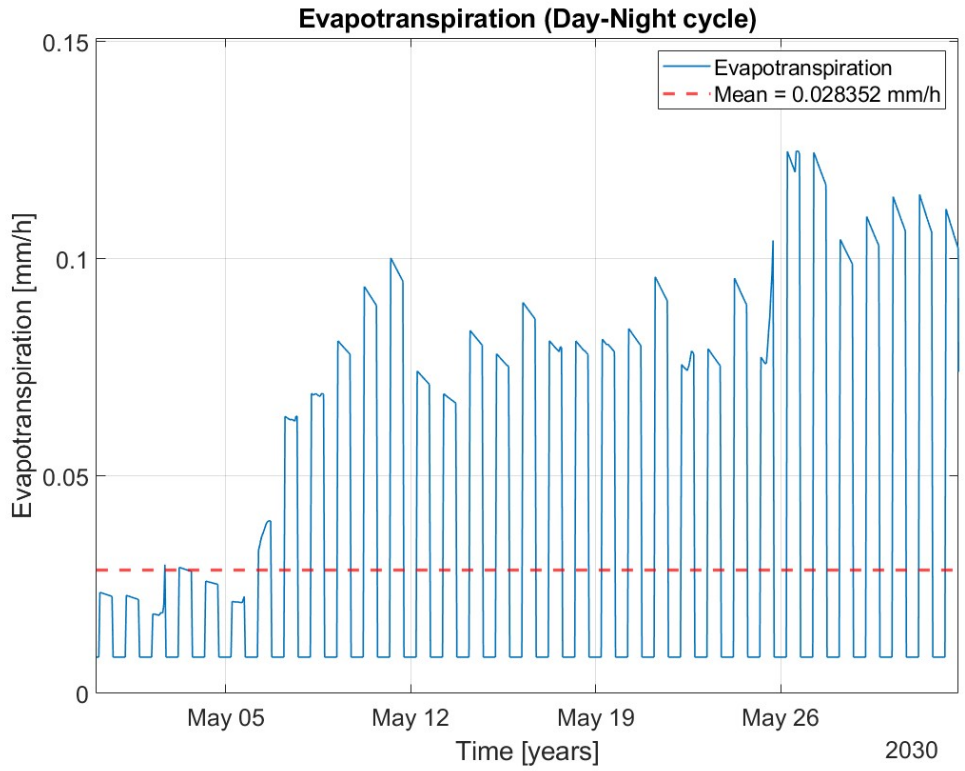

Figure 4.10: Hourly time series of evapotranspiraton over an example month with $K_c = 0.5$.

Figure 4.10 shows the behavior of the evapotranspiration over a month. Here is possible to see the day and night changes, where the daily cycles are marked. It is possible to see that at the beginning of the month, the evaporation rates during the day where low and then started to increase as the month passed. In particular one can see that every night the evapotranspiration come to its minimum. Additionally, the rates over the day are also not the same, they vary depending on the hour of the day and the factors like temperature and soil moisture.

Furthermore, a better appreciation of the evapotranspiration deficit index (EDI) can be seen in the following figure, where the daily changes, the peaks and the constant values during a year are better represented.

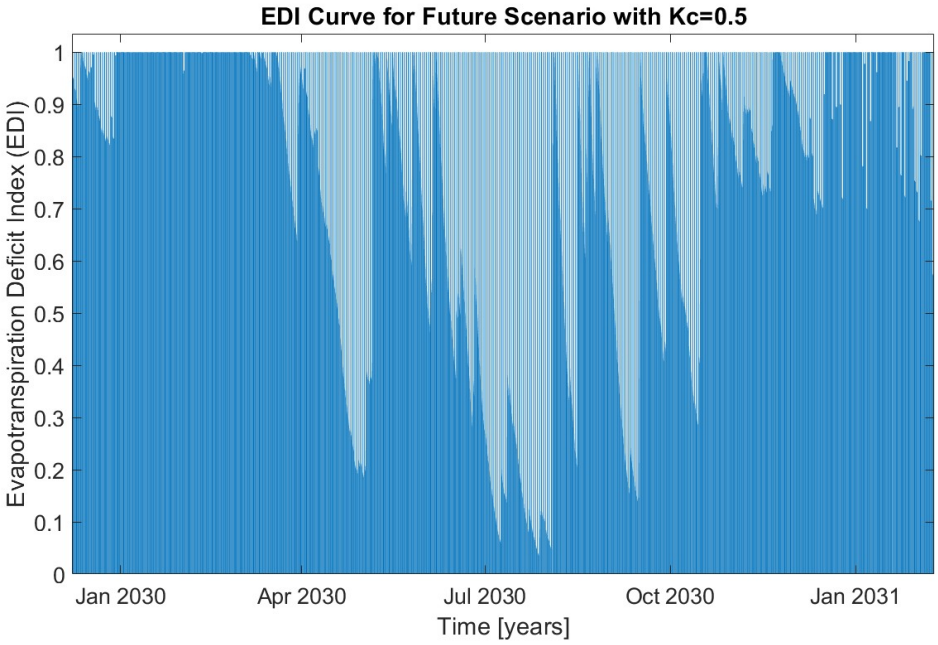

Figure 4.11: Evapotranspiraton Deficit Index (EDI) over the example year.

From Figure 4.11 one can see the seasonal variation of the deficit in evapotranspiration across the whole year. During the summer period there is a noticeable decrease in the EDI because of the increment of the day-light hours, which suggest periods of higher evapotranspiration and also an increment in the precipitation during that time. On the contrary at the beginning and at the end of the Figure 4.11 a higher deficit index is appreciable. It is related also to the seasons and the daylight, highlighting dryer periods with lower evapotranspiration rates.

Soil Moisture Deficit

After knowing the evapotranspiration values of the Green Roof for the different K_c values in the future scenario, it is also important to know how many hours and days one has a soil moisture deficit and the soil needs to be irrigated.

Case	Hourly scale		Daily scale	
	Total number of hours	Number of $\frac{hours}{year}$	Total number of days	Number of $\frac{days}{year}$
1	85302	1312	3375	52
2	140350	2159	5947	91
3	157556	2424	6791	104
4	101633	1564	4588	71

Table 4.4: Number of hours and days with a soil moisture lower than 30% of the soil moisture at field capacity (sfc)

Table 4.4 shows the number of hours and days on which the soil moisture value is lower than the one at the 30% of the field capacity (sfc), meaning lower than 0.156. In general terms is possible to see that both number of hours and days are bigger with a higher crop coefficient in comparison to the ones with a lower K_c. This shows the difference in terms of necessity of irrigation between a scare succulent vegetation and a herbaceous one with the same nZ_r. Case 4, shows that if the nZ_r gets doubled, the days and hours bellow the 30% of the field capacity get reduced in 65% with respect to case 3 that has the same vegetation.

4.2.2 Simulated Discharge (Q_s)

The principal output of the simulation is the value of the discharge that the Green Roof is able to evacuate after a precipitation event. In this case, the model was run for both daily and hourly scales for the different cases as can be seen in the Table 4.5.

Case	$Q_s[\frac{mm}{h}]$
1	0.074
2	0.067
3	0.065
4	0.058

Table 4.5: Mean discharge (Q_s) for the Future Scenario.

Days with Simulated Discharge (Q_s)

As said before in the section 3.3, the Q_s is the amount of water that exits the Green Roof as leakage and does not get absorbed by the vegetation or evaporated back into the atmosphere. For its simulation, the process previously reported in the chapter 3 was performed and the main aim of this process is to know how much

water is retained by the Green Roof, how much is evacuated and on how many days does does one have this situation.

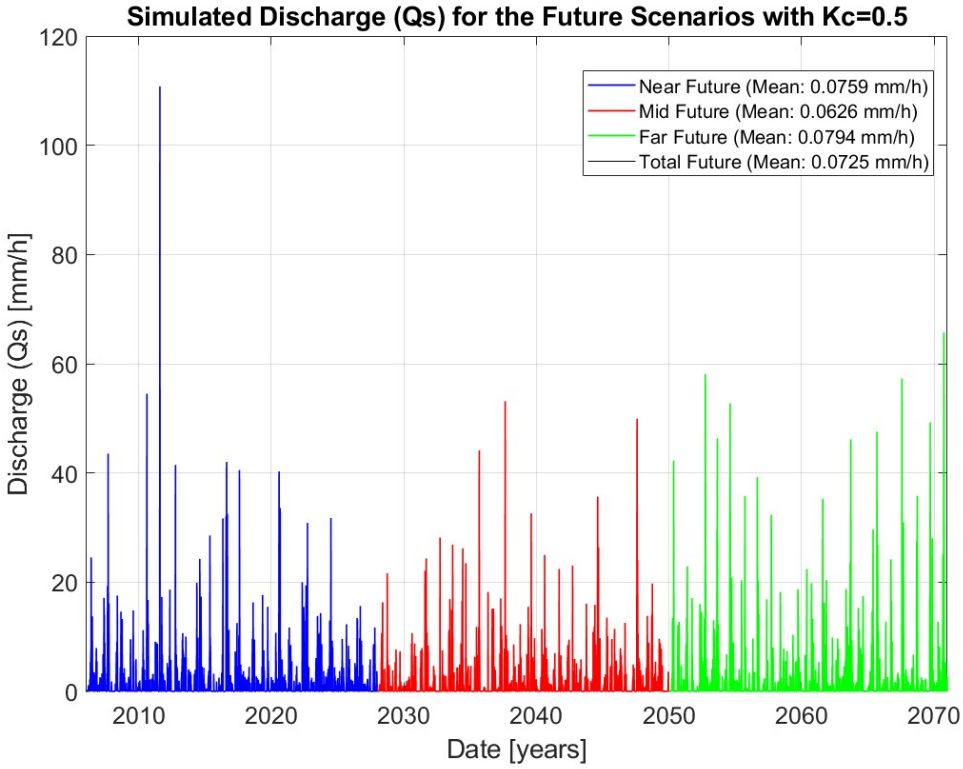

Figure 4.12: Hourly scale time series of simulated discharge Q_s for the future periods with $K_c = 0.5$.

From Figure 4.12 is possible to see that the mean discharge in the Near and Far futures is very similar for the case when $K_c = 0.5$, while in the Mid future it is relatively smaller. The data used for this graph is on an hourly scale, and speaking in terms of hours, there are 34754 hours where there was a discharge higher than zero. At the same time, on a daily scale, there are 4011 days on which there is a daily simulated discharge higher than zero. Nevertheless, there are many values that the simulation computes that are not 100% correct. Those values are very low for a daily or even an hourly scale, where physically meaning they do not have any sense. That's why for both hourly and daily scales one has the values of the discharge higher than a threshold of 1 mm for both day and hour. The results are shown in the Table 4.6.

	Hours			**Days**		
Case	$Q_s = 0mm$	$Q_s > 0mm$	$Q_s > 1mm$	$Q_s = 0mm$	$Q_s > 0mm$	$Q_s > 1mm$
1	535030	34754	10530	19730	4011	3337
2	540454	29330	9436	20364	3377	2877
3	542106	27678	9104	20560	3181	2732
4	544861	24923	8116	20900	2841	2443

Table 4.6: Number of hours and days when one has $Q_s = 0mm$,$Q_s > 0mm$ and $Q_s > 1mm$.

From the table is possible to infer that as the crop coefficient K_c increases, the production of discharge decreases. This means, that the vegetation absorbs and help to retain more water in the soil bucket and does not let it pass through. In this case the type of vegetation plays a key role, where the succulent vegetation (with a low K_c, in this case 0.5) lets more water to infiltrate due to their ability to store water. On the contrary herbaceous vegetation, referring to a higher K_c (for this simulation equal to 1), need more constant irrigation, so they retain less water and as can be seen in the Table 4.6 decrease the number of hours and days on which there is discharge exiting the system.

Moreover, an increase in the active soil depth (nZ_r) correlates with an increase in the duration of periods with zero discharge. This phenomenon occurs because a deeper root zone allows for greater water retention within the soil profile, thereby reducing immediate surface discharge. This effect is illustrated in the last two rows of the table, where the crop coefficient (K_c) is constant, yet nZ_r is doubled. This modification results in a reduction of discharge generation by approximately 11% in both number of hours and days.

	Maximum Q_s value			
Case	$Q_s[\frac{mm}{h}]$	Date and Hour	$Q_s[\frac{mm}{day}]$	Date
1	110.77	6/08/2011 14:00	311.05	6/08/2011
2	110.69	6/08/2011 14:00	310.09	6/08/2011
3	110.65	6/08/2011 14:00	309.68	6/08/2011
4	110.65	6/08/2011 14:00	309.68	6/08/2011

Table 4.7: Maximum Q_s for both Hourly and Daily scales with different K_c and nZ_r values.

From the Table 4.8 and Table 4.7 one can see that the maximum simulated discharge is on the 6/08/2011 and also that the changes on the discharge by varying the coefficients K_c and nZ_r is not that big. Even though there is a reduction when there is a higher K_c, most of the water gets evacuated as Leakage. The intensity of

the event was so high, that from the 110.88 mm that felt during that hour, 110.77 mm were discharged out of the Green Roof. Most of that evacuated water was in form of excess saturation surface runoff.

Case	Annual Averages			Other Metrics		
	Precip $[\frac{mm}{y}]$	ET $[\frac{mm}{y}]$	$Q_s[\frac{mm}{y}]$	Days with $Qs = 0[\frac{d}{y}]$	Hours with $Qs = 0[\frac{d}{y}]$	$\Psi[-]$
1	885	239	646	308	8224	0.73
2	885	298	587	313	8303	0.66
3	885	317	568	315	8328	0.64
4	885	380	505	321	8373	0.57

Table 4.8: Comparison of hydrological balance variables for different cases on an hourly scale for the Future Scenario.

Regarding the simulated discharge, Table 4.8 shows that the annual Q_s decreases as the K_c coefficient increases. For a substrate with $nZ_r = 40mm$, used in cases 1, 2, and 3, a reduction in discharge of 9% to 12% is observed in cases 2 and 3 when compared to case 1. In terms of the Runoff coefficient (Ψ) , the coefficient gets reduced as the K_c increases, showing a better water retention as one changes cases. The reduction from case 1 to case 4 is significant, as expected due to the change in the K_c coefficient and the duplication of the soil substrate's thickness.
It is also interesting to see the increment on the number of days and hours without a discharge, showing that light rains can be attenuated on approximately 12 more days per year when changing from case 1 to case 4.

Flow Duration Curve (FDC)

In this section, the simulation was also performed for each of the three future scenario periods mentioned before. Each of the graphs shows the four plots of the cases mentioned in the Table 4.1. For illustration of the results just the final FDC that contains the plot of the whole period FDC for each of the four cases is going to be shown in this section.

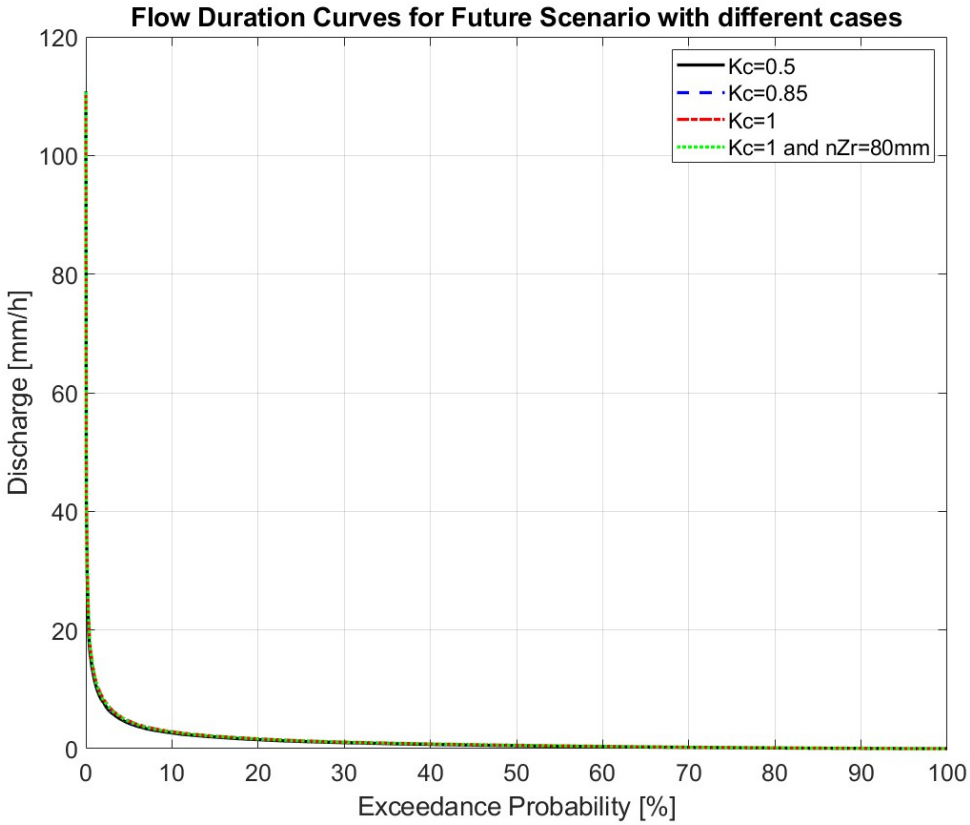

Figure 4.13: FDC for the whole future scenario with the four cases.

For instance, Figure 4.13 is very steep at the begging of the exceedance probability and then, when it starts to increase, the curve flattens. This steep behaviour at the beginning of the curve indicates that the high discharge rates are uncommon and those that happen are a on a very small portion of time in comparison to the analyzed period. From the beginning of the curve in the y axis, one can see that the highest discharge rate is around $110[mm/h]$ and corresponds to a very rare probability of exceedance. On the other hand, the flat behaviour that predominates on the curve tells that lower discharge rates occur more frequently. Particularly, from 80% on, the discharge is very low indicating that for most of the time, the discharge rate is significantly small or does not discharge anything at all.

Flow Accumulation Curve (FAC)

The aim of this figure is to illustrate how does the system reacts to the amount of water that it receives. It can be seen that the curve has a slower and gradual increase along the years, which suggest good retention in the Green Roof, with a

slow release of water over time. In some parts one can see that there are steeper slopes, meaning that there was a significant precipitation event that added much water to the cumulative curve in a small period of time. Overall, one can say that the system effectively controls the runoff in the Green Roof due to the gradually rising of the curve. Is clear that the scale of the curve is in years, while in the case of months or days, one can see more behaviour on the cumulative volume. Furthermore, the difference between the cumulative discharge and cumulative precipitation indicates the amount of water that has been either evaporated from the soil or transpired by the vegetation.

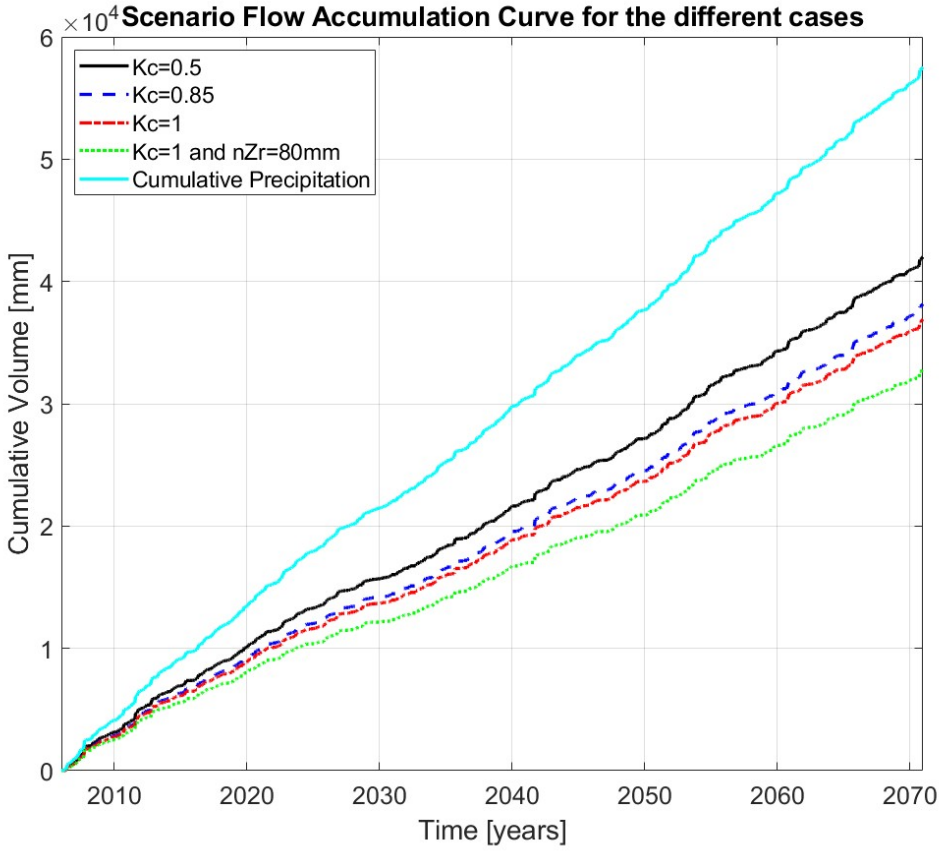

Figure 4.14: Flow Accumulation Curve (FAC) for the different cases.

Simulated Discharge (Q_s) for example year (2030-2031)

In order to understand on a smaller scale the behaviour of the model, a random year was selected along the sample of the future scenario. In this case the selected year was 2030, that falls into the Mid Future period of the Future Scenario division.

The aim is to illustrate how the behaviour of the simulated discharge in the Green Roof changes according to the seasonality of the weather.

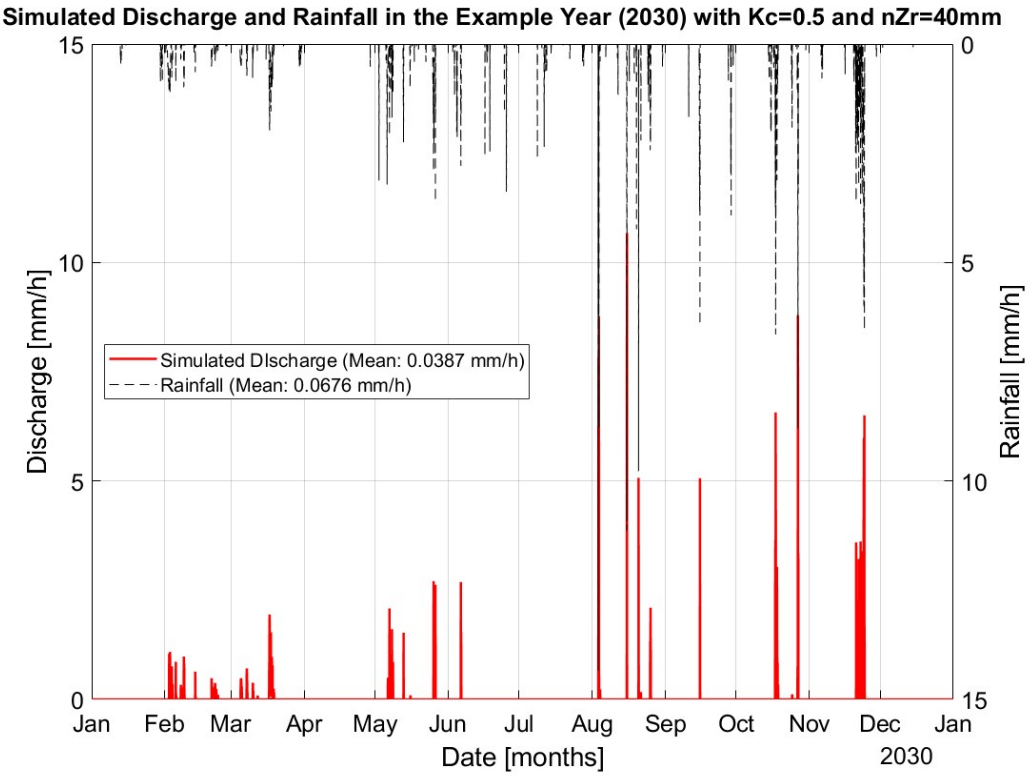

Figure 4.15: Q_s and Rainfall for the example year with $K_c = 0.5$.

Furthermore, from the Figure 4.15 is possible to see both discharge and rainfall at the same time, where one can notice that on the days of peaks on the precipitation, one will also have peaks on the discharge. Those peaks appear in the periods of the year, when the precipitation in the city of Turin tends to be higher. Those periods of more probability of precipitation are from April to June and from August to November.

Days with Precipitation and no discharge (Q_s)

After analyzing the simulated data performed by the model is important to see in comparison to the precipitation, how many times there was no discharge simulation while it rained.

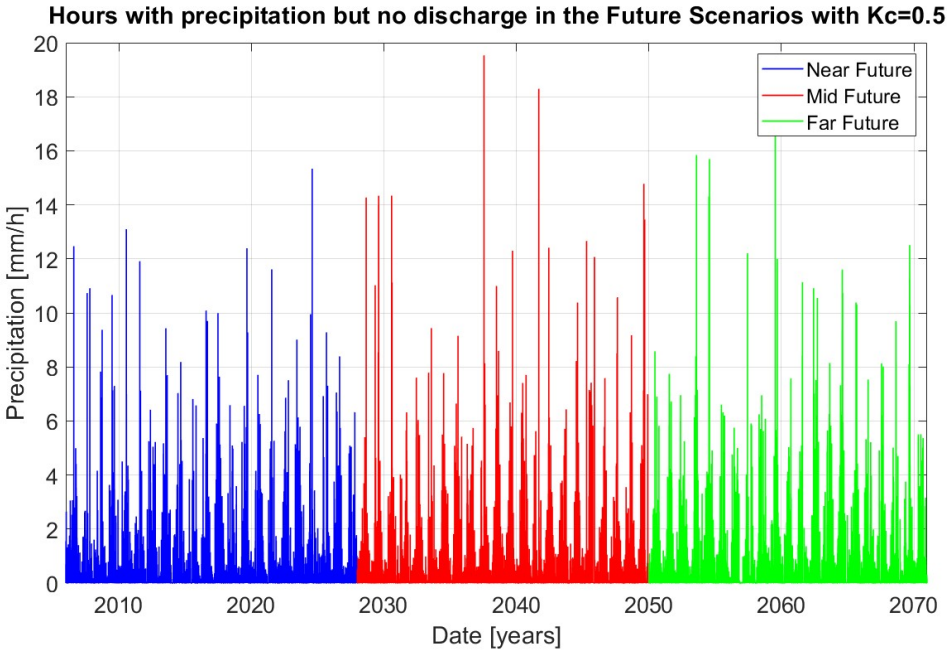

Figure 4.16: Hourly scale time series of precipitation and no Q_s for the future periods.

In Figure 4.16 is possible to see the hours on which there was precipitation recorded but no discharge was simulated by the model.It is worth highlighting that this graph is made for Case 1, with a K_c of 0.5 and a nZ_r of 40mm. From a daily point of view, for this case, a total amount of 6291 days, out of 23741 (which are the 65 years), have recorded days with precipitation higher than zero and no discharge. Nevertheless, is worth mentioning that as this is a scenario case, there are values that are considered higher than zero, but cannot be counted as rain because the order of magnitude is not big enough. That is why, is also valuable to highlight that the total amount of days recorded with a daily precipitation higher than $1mm$ is 5304 as can be seen in Table 4.9. The latter means that on 28.4% of rainy days, no runoff is generated, meaning that the green roof is able to retain the precipitation. Speaking in terms of hours, one can see that from the hourly scale simulation it states that in 2720 times, from a total of 569784 hours, there was the same condition presented where there is no discharge in precipitation events higher than $1mm$. In hourly scale, the number of hours with precipitation higher than $1mm$ is equal to 14202.

Case	**Total** $[days]$	$P > 1[\frac{mm}{day}]$	$P > 1[\frac{mm}{day}]$ & $Q_s = 0[\frac{mm}{day}]$
1	23741	5304	1504
2			2013
3			2181
4			2519

Table 4.9: Overview of time periods with precipitation but no discharge for $K_c = 0.5$.

Figure 4.16 illustrates the time periods during which precipitation was recorded, but no discharge was simulated by the model. This analysis is based on a model parameterized with a crop coefficient (K_c) of 0.5 and an active soil depth (nZ_r) of 40 mm.

Comparing this to the total number of rainfall days, it can be seen that the Green Roof is able to retain a significant portion of the precipitation that falls on it. Specifically, the results indicate that for approximately 26.5% of the total days, there is rainfall and no discharge is observed. This suggests that the substrate and vegetation are effectively absorbing the water, preventing immediate runoff. At the hourly scale, the Green Roof demonstrates even more granular water retention, with no discharge occurring in approximately 12% of the simulated hours with precipitation. This highlights the roof's capacity to regulate water flow, likely through a combination of infiltration into the substrate, water uptake by vegetation, and evapotranspiration.

4.3 Comparison between Historical and Future Simulations

In this section there is a comparison between both the results of the Historical and Future scenarios, in terms of Precipitation, Evapotranspiration, Simulated discharge Q_s and the Runoff coefficient Ψ.

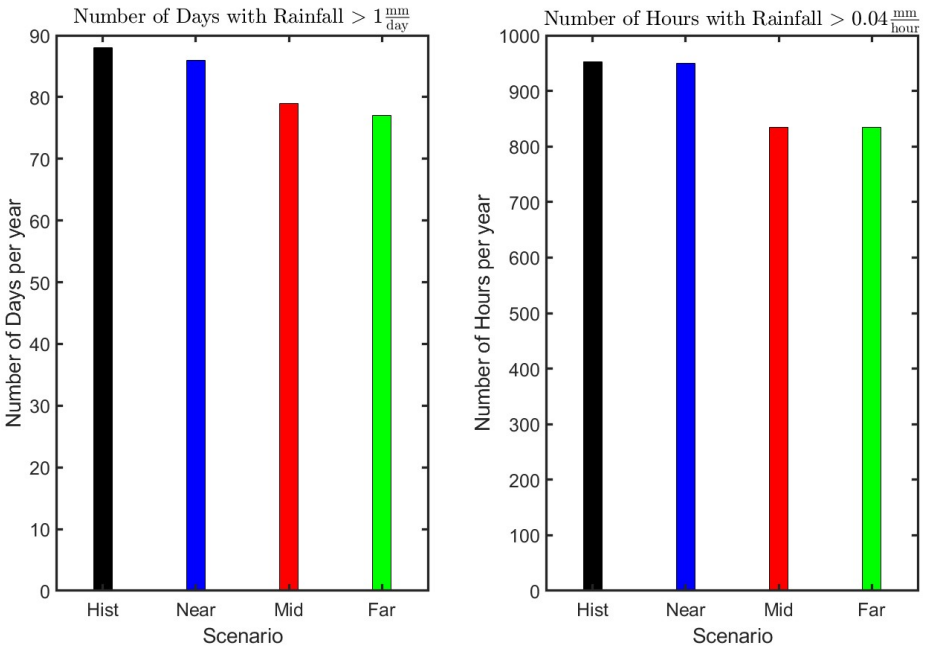

Figure 4.17: Mean number of days and hours per year with rainfall intensity higher than $1\frac{mm}{day}$.

Based on Figure 4.17 is possible to see the behavior of the system as the Plan for Green Infrastructure describes in [4]. The rainy days per year are decreasing due to the climate change and even though the reduction in terms of percentage between the Historical simulation and the Far future one is of around 13%, it is a significant value. Additionally, in terms of peaks, the Plan for Green Infrastructure expects that in the coming future, there will be stronger rain events. This trend is evident in Figure 4.1 and Figure 4.6, where the peaks in the Future scenario are expected to be stronger than the ones in the Historical one.

Case	Scenario	Precip $[\frac{mm}{y}]$	$ET[\frac{mm}{y}]$	$Q_s[\frac{mm}{y}]$	$\Psi[-]$
Case 1	Historical	900.01	244.65	654.77	0.73
	Future	885.19	238.54	646.38	0.73
Case 2	Historical	900.01	314.02	585.47	0.65
	Future	885.19	297.73	587.20	0.66
Case 3	Historical	900.01	336.64	562.88	0.63
	Future	885.19	317.03	567.89	0.64
Case 4	Historical	900.01	396.08	502.74	0.56
	Future	885.19	379.72	504.94	0.57

Table 4.10: Comparison of Precipitation, ET, Q_s, and Ψ between Historical and Future Scenarios across the different cases.

According to Table 4.10 is possible to see that both Historical and Future scenarios have the same trend, well the evapotranspiration increases more or less at the same rate and the discharge decreases simultaneously as well. Interesting is that the simulated discharge was higher for the historical scenario in the Case 1, but in the following Cases the future scenario surpassed the historical one. That can also be evidenced in the runoff coefficient, where apart from Case 1, the future scenario is 0.01 ahead of the historical one. Is also noticeable that the evapotranspiration difference between Case 1 and Case 4 is around 60%. Comparing it with the case 3, where the active soil depth is the same and what changes is the type of vegetation, it can be seen that the evapotranspiration increases in 35% approximately in both scenarios. On the contrary, the simulated discharge gets reduced as the K_c increases and gets more reduced in the case where the nZ_r gets doubled. Nevertheless, the maximum discharge reduction is of 35% and is between Case 1 and Case 4 being almost half, in percentage terms, of that of the change in evapotranspiration.

Chapter 5

Conclusions

The primary objective of this study was to simulate the performance of Green Roof systems in Turin for mitigating stormwater runoff. This was achieved by conducting a series of hydrological simulations using the Ecohydrological Streamflow Model (EHSM), as developed by F. Viola, D. Pumo, and L.V. Noto in [33]. The simulation outcomes show the system's behavior under future climatic conditions, demonstrating the potential benefits in terms of runoff attenuation and reduction in peak flow magnitudes after its implementation.

Regarding the data calibration, is possible to see that both Figure 3.6 and Figure 3.3 reveal that the biases for the two variables are significantly high. In the case of precipitation, the bias is estimated as a ratio that then gets multiplied for each value for the correction. The maximum ratio reaches a magnitude of 3 units, which, being a multiplicative correction factor, is considered substantially high. Similarly, for temperature, the bias values are also elevated, with corrections approaching 4 degrees over the course of a single month. The magnitude of these biases indicates the need for an alternative bias correction method, as the current approach results in correction factors that are excessively large.

Analysing the results from Table 4.10, it is apparent that the statement from the Plan for Green Infrastructure is accurate, showing that even if in the historical scenario there was more mean precipitation per year, its runoff coefficient was lower in most cases. Despite the small difference between the runoff coefficients in the historical and future scenarios, the historical scenario suggests a higher potential for water retention and a lower discharge generation. This difference is closely related to the intensity and occurrence of precipitation events. While the future scenario is characterized by a lower average annual precipitation, the rainfall events tend to be more intense, saturating the system faster and resulting in the generation of more discharge.

Results suggest that in all cases there is a percentage of water that gets attenuated by the Green Roof. This is a significant improvement over normal roofs, considering

that for the case with the lowest runoff coefficient, the Green Roof is able to attenuate 35% of the rain that falls over it. The case that reaches to reduce the precipitation the most is case 4, where 43% of the fallen rain gets retained by the Green Roof structure. Consequently, the selection of the better case will depend on the type of building on which the Green Roof will be placed on, due to the loads that it can transfer to the structure and weather it is a new or an old building. In terms of the load that the Green Roof applies to the roofing structure it is around $5\frac{kN}{m^2}$ in roof without trees and crowd loads according to [2], and for this cases the maximum weight of the substrate layer is $3.67\frac{kN}{m^2}$ as seen in Table 3.1.

It is evident that succulent vegetation (Cases 1 and 2) requires less irrigation and can survive extended periods without water. Given this, and taking into account the need to attenuate intense precipitation events, Case 2 presents an optimal solution for the Green Roof system. When compared to Case 3, which has the same substrate depth (nZ_r) but a different vegetation type, the runoff coefficient shows minimal variation, whereas the irrigation requirements of the vegetation change significantly. That is why, for the roof, with no special structural design or adjustments, the recommended solution is to implement the Green Roof configuration as defined in Case 2.

Appendix A

Figures of the simulations for each of the future scenario periods and cases.

A.1 EDC

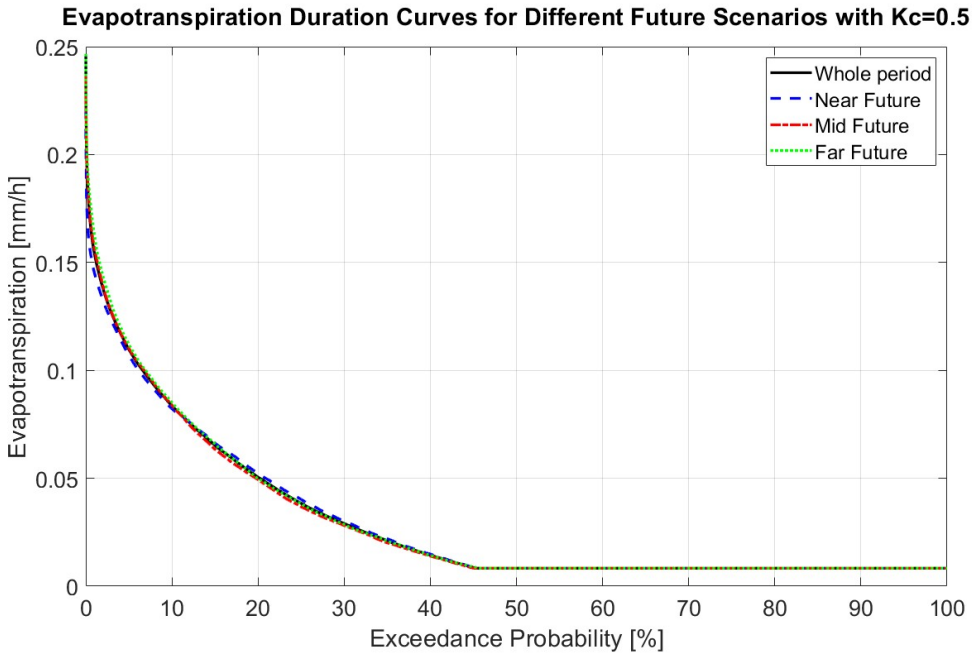

Figure A.1: EDC with $K_c = 0.5$.

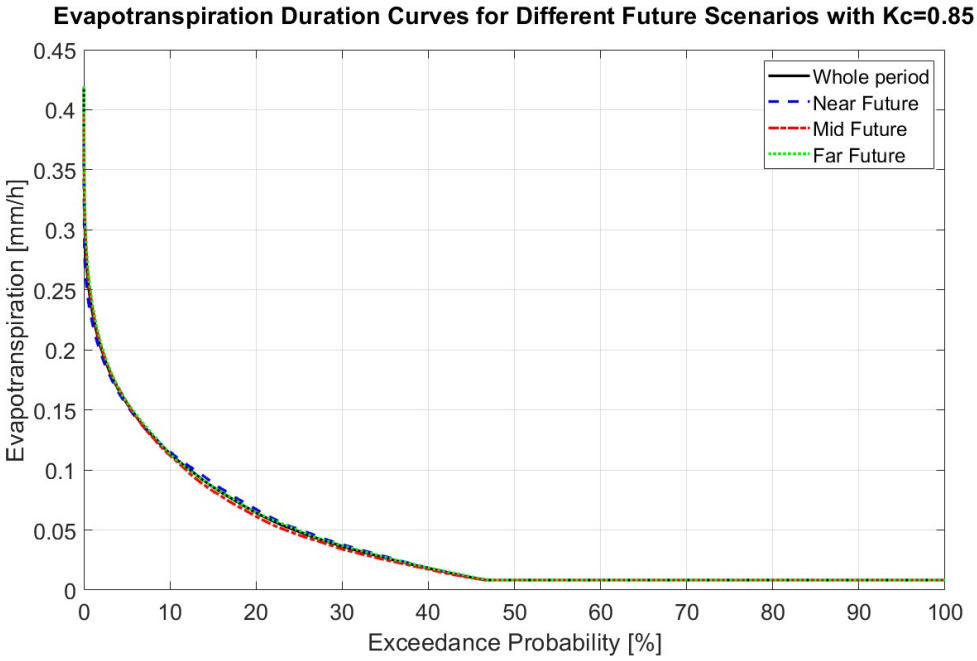

Figure A.2: EDC with $K_c = 0.85$.

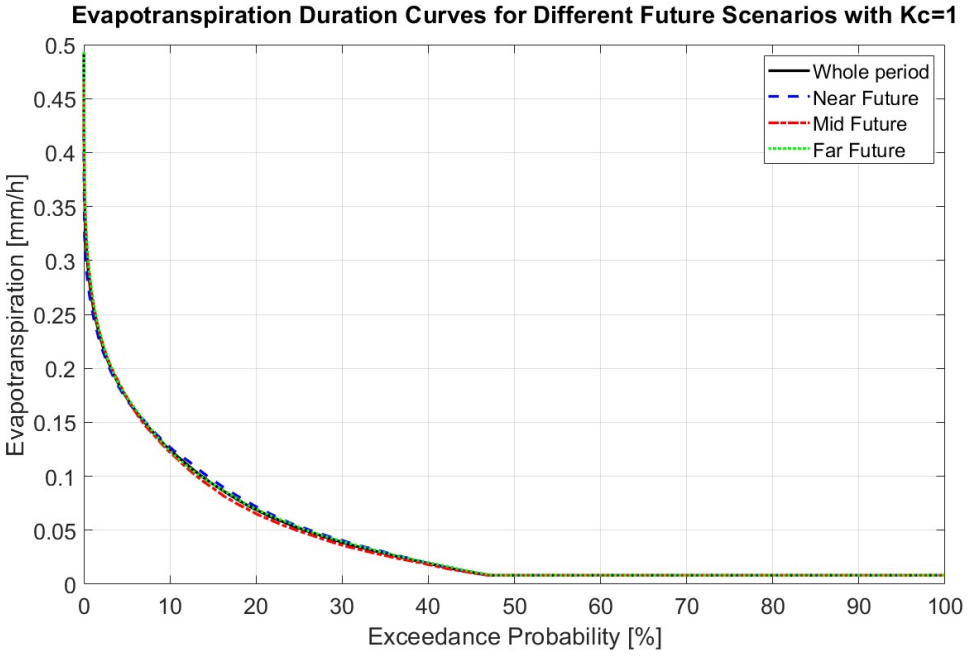

Figure A.3: EDC with $K_c = 1$.

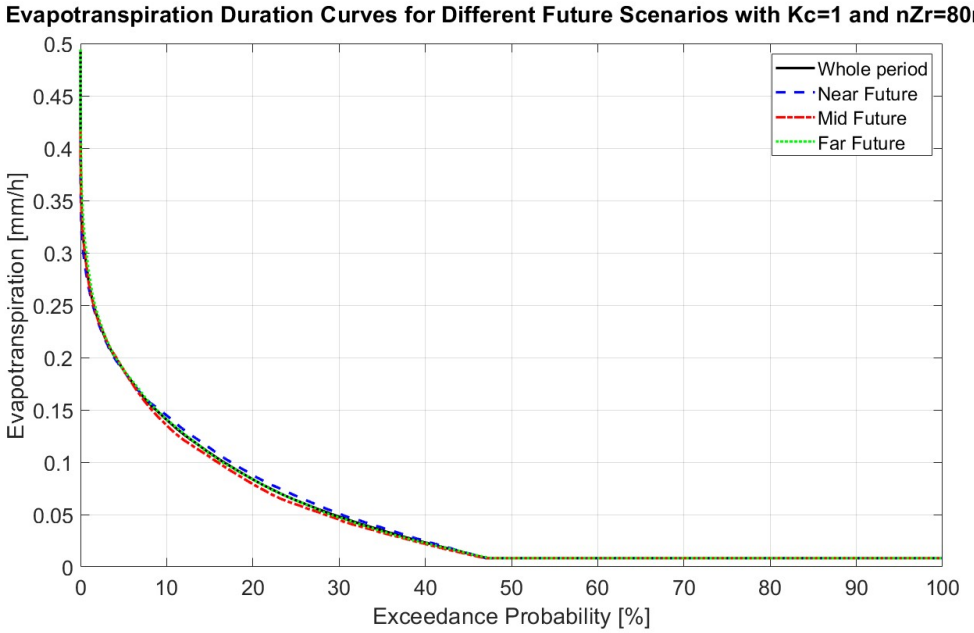

Figure A.4: EDC with $K_c = 1$ and $nZ_r = 80mm$.

A.2 FDC

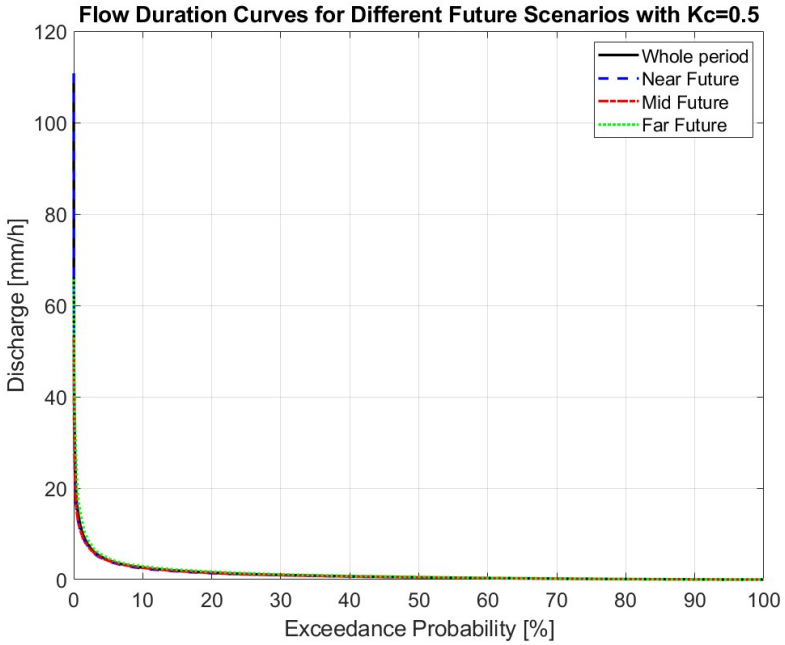

Figure A.5: FDC with $K_c = 0.5$.

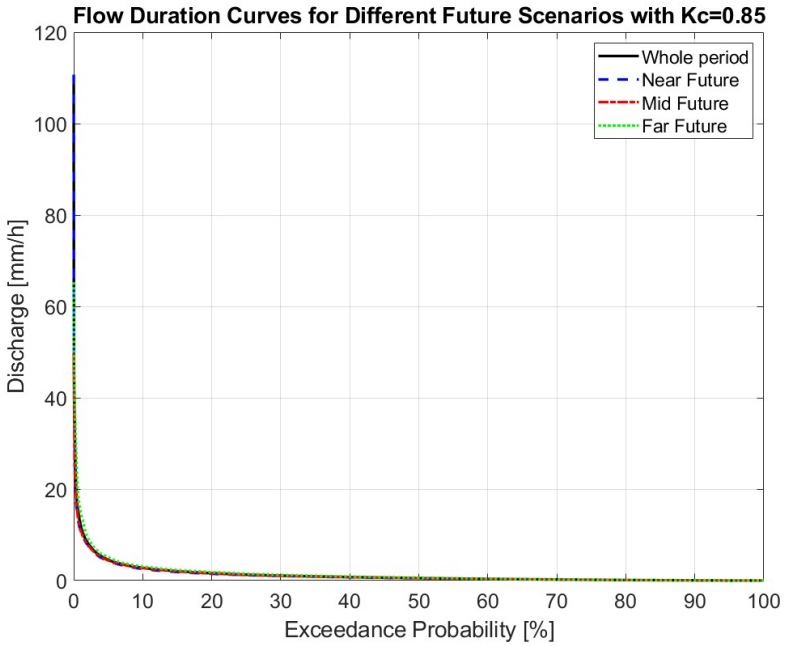

Figure A.6: FDC with $K_c = 0.85$.

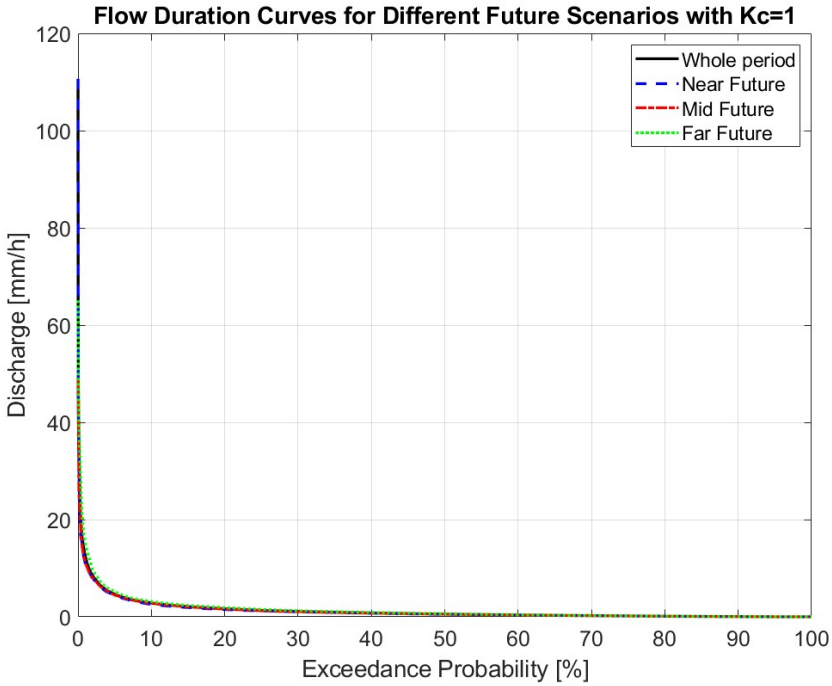

Figure A.7: FDC with $K_c = 1$.

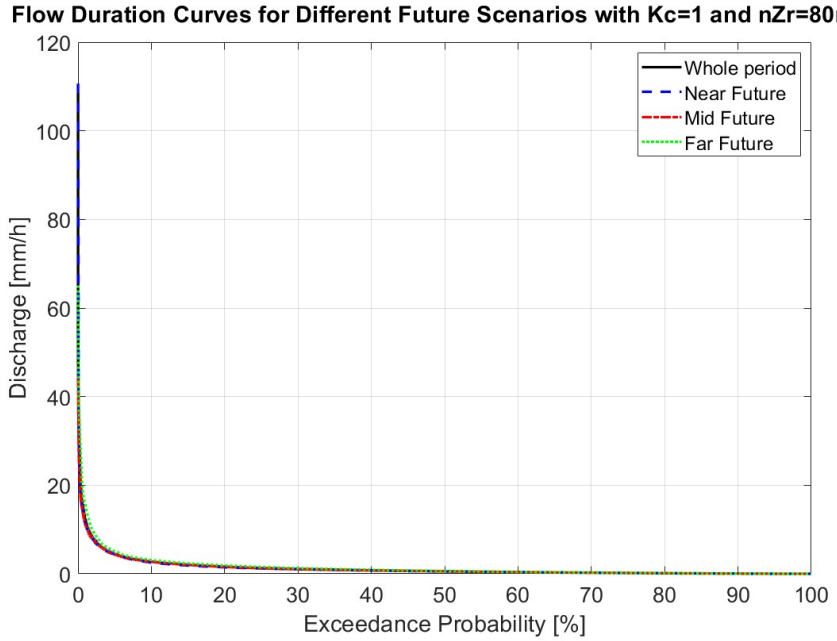

Figure A.8: FDC with $K_c = 1$ and $nZ_r = 80mm$.

A.3 Comparison of Results across cases

Case	**Scenario**	**Precip** $[\frac{mm}{y}]$	$ET[\frac{mm}{y}]$	$Q_s[\frac{mm}{y}]$	$\Psi[-]$
Case 1	Historical	900.01	244.65	654.77	0.73
	Near	916.44	240.50	675.25	0.74
	Mid	796.88	236.88	559.24	0.70
	Far	944.95	238.07	706.06	0.75
Case 2	Historical	900.01	314.02	585.47	0.65
	Near	916.44	304.98	610.79	0.67
	Mid	796.88	292.38	503.82	0.63
	Far	944.95	295.36	648.79	0.69
Case 3	Historical	900.01	336.64	562.88	0.63
	Near	916.44	326.19	589.60	0.64
	Mid	796.88	310.53	485.71	0.61
	Far	944.95	313.80	630.34	0.67
Case 4	Historical	900.01	396.08	502.74	0.56
	Near	916.44	390.49	524.49	0.57
	Mid	796.88	370.43	425.03	0.53
	Far	944.95	377.19	566.11	0.60

Table A.1: Comparison of Precipitation, ET, Q_s, and Ψ between Historical and the different Future Scenarios across the different cases.

Bibliography

[1] Walter Leal Filho, Anabela Marisa Azul, Luciana Brandli, Pinar Gökçin Özuyar, and Tony Wall. *Sustainable Cities and Communities*. Springer Cham, 2020 (cit. on pp. 1, 3).

[2] Bridget Woods Ballard, Steve Wilson, Helen Udale-Clarke, Sue Illman, Tamasine Scott, Richard Ashley, and Richard Kellagher. *The SuDS Manual*. London: CIRIA, 2015. ISBN: 978-0-86017-760-92 (cit. on pp. 1, 4–9, 11–13, 65).

[3] Comune di Torino. *Piano Strategico dell'Infrastruttura Verde*. Accessed: 14-September-2024. 2020. URL: https://servizi.comune.torino.it/consiglio/prg/documenti1/atti/allegati/202002957_1tc.pdf (cit. on p. 2).

[4] Comune di Torino. *Climate Resilience Plan*. [Accessed: 23-September-2024]. 2020. URL: http://www.comune.torino.it/ambiente/bm~doc/resilienza-climatica_en.pdf (cit. on pp. 2, 62).

[5] *Stormwater Best Management Practices*. Accessed: Sep. 19, 2024. Southwestern Pennsylvania Commission. 2024. URL: https://spcwater.org/topics/stormwater-management/stormwater-best-management-practices-2/ (cit. on p. 4).

[6] A.E. Barbosa, J.N. Fernandes, and L.M. David. «Key issues for sustainable urban stormwater management». In: *Water Research* 46.20 (2012). Special Issue on Stormwater in urban areas, pp. 6787–6798. ISSN: 0043-1354. DOI: https://doi.org/10.1016/j.watres.2012.05.029. URL: https://www.sciencedirect.com/science/article/pii/S0043135412003569 (cit. on p. 4).

[7] C.Y. Jim. «An archaeological and historical exploration of the origins of green roofs». In: *Urban Forestry Urban Greening*. 27 (2017), pp. 32–42 (cit. on p. 10).

[8] Joost van Hoof and Froukje van Dijken. «The historical turf farms of Iceland: Architecture, building technology and the indoor environment». In: *Building and Environment* 43.6 (2008), p. 1023.1030 (cit. on p. 10).

[9] C.Y. Jim. «Green roof evolution through exemplars: Germinal prototypes to modern variants». In: *Sustainable Cities and Society* 35 (2017), pp. 69–82. ISSN: 2210-6707. DOI: https://doi.org/10.1016/j.scs.2017.08.001. URL: https://www.sciencedirect.com/science/article/pii/S2210670717306121 (cit. on p. 11).

[10] F Abass, L H Ismail, I A Wahab, and A A Elgadi. «A Review of Green Roof: Definition, History, Evolution and Functions». In: *IOP Conference Series: Materials Science and Engineering* 713.1 (Jan. 2020), p. 012048. DOI: 10.1088/1757-899X/713/1/012048. URL: https://dx.doi.org/10.1088/1757-899X/713/1/012048 (cit. on p. 11).

[11] Lynne Bridge. «40 The Roof Gardens, Kensington, London». In: *Gardens landscapes in historic building conservation*. John Wiley Sons, Ltd, The Atrium, Southern Gate, Chichester West Sussex, PO19 8SQ, UK, Dec. 2014, p. 397 (cit. on p. 14).

[12] Société Nationale d'Horticulture de France. *Le jardin impossible et les 30 ans du Jardin Atlantique*. Online. Accessed: Aug. 9, 2024. 2024. URL: https://www.snhf.org/les-30-ans-du-jardin-atlantique/ (cit. on p. 15).

[13] La Petite Rosa. *La coulée verte*. Online. Accessed: Aug. 9, 2024. 2024. URL: https://www.hotel-lapetiterosa.fr/es/places/la-coulee-verte/ (cit. on p. 15).

[14] Adrian Ballese. *Die Waldspirale in Darmstadt*. Online. Accessed: Aug. 9, 2024. 2002. URL: https://hundertwasser.com/architektur/arch120_die_wald-spirale_von_darmstadt_1547 (cit. on p. 16).

[15] Greenroofs. *Rockefeller Center Roof Gardens*. Online. Accessed: Aug. 9, 2024. URL: https://www.greenroofs.com/projects/rockefeller-center-roof-gardens/7 (cit. on p. 17).

[16] Sarah Milligan. *This living roof is a home for plants and wildlife – right in the city*. Online. Accessed: Aug. 9, 2024. 2023. URL: https://www.rewildingmag.com/living-roof-california-academy-of-sciences/ (cit. on p. 17).

[17] Earth Resources Observation and Science (EROS) Center. *Chicago City Hall aerial*. Online. Accessed: Aug. 9, 2024. 2019. URL: https://www.usgs.gov/media/images/chicago-city-hall-aerial (cit. on p. 18).

[18] Xero Flor America. *Ford Motor Company's River Rouge Truck Plant*. Online. Accessed: Aug. 9, 2024. 2007. URL: https://www.greenroofs.com/projects/ford-motor-companys-river-rouge-truck-plant/ (cit. on p. 18).

[19] MITSUI SUMITOMO INSURANCE COMPANY. *Mitsui Sumitomo Insurance × Planetary Health Resilience*. Online. Accessed: Aug. 9, 2024. URL: https://www.sumitomo.gr.jp/english/act/social-issue/ms-ins/ (cit. on p. 19).

[20] Green Roofs. *ACROS Fukuoka Prefectural International Hall*. Online. Accessed: Aug. 9, 2024. URL: https://www.greenroofs.com/projects/acros-fukuoka-prefectural-international-hall/ (cit. on p. 20).

[21] Elena Cristiano, Francesco Lai, Roberto Deidda, and Francesco Viola. «Management strategies for maximizing the ecohydrological benefits of multilayer blue-green roofs in mediterranean urban areas». In: *Journal of Environmental Management* 343 (2023), p. 118248. ISSN: 0301-4797. DOI: https://doi.org/10.1016/j.jenvman.2023.118248. URL: https://www.sciencedirect.com/science/article/pii/S0301479723010368 (cit. on pp. 21, 27, 37, 38).

[22] Dario Pumo, Antonio Francipane, Francesco Alongi, and Leonardo V. Noto. «The potential of multilayer green roofs for stormwater management in urban area under semi-arid Mediterranean climate conditions». In: *Journal of Environmental Management* 326 (2023), p. 116643. ISSN: 0301-4797. DOI: https://doi.org/10.1016/j.jenvman.2022.116643. URL: https://www.sciencedirect.com/science/article/pii/S0301479722022162 (cit. on p. 22).

[23] Tim Busker, Hans de Moel, Toon Haer, Maurice Schmeits, Bart van den Hurk, Kira Myers, Dirk Gijsbert Cirkel, and Jeroen Aerts. «Blue-green roofs with forecast-based operation to reduce the impact of weather extremes». In: *Journal of Environmental Management* 301 (2022), p. 113750. ISSN: 0301-4797. DOI: https://doi.org/10.1016/j.jenvman.2021.113750. URL: https://www.sciencedirect.com/science/article/pii/S0301479721018120 (cit. on p. 24).

[24] Mohammad A. Alim, Sayka Jahan, Ataur Rahman, Mohammad Ataur Rahman, Mark Liebman, Brad Garner, Robert Griffith, Merran Griffith, and Zhong Tao. «Experimental investigation of a multilayer detention roof for stormwater management». In: *Journal of Cleaner Production* 395 (2023), p. 136413. ISSN: 0959-6526. DOI: https://doi.org/10.1016/j.jclepro.2023.136413. URL: https://www.sciencedirect.com/science/article/pii/S0959652623005711 (cit. on p. 24).

[25] Satish Kumar, Ravi Kumar Guntu, Ankit Agarwal, Vasant Govind Kumar Villuri, Srinivas Pasupuleti, Deo Raj Kaushal, Ashwin Kumar Gosian, and Axel Bronstert. «Multi-objective optimization for stormwater management by green-roofs and infiltration trenches to reduce urban flooding in central

Delhi». In: *Journal of Hydrology* 606 (2022), p. 127455. ISSN: 0022-1694. DOI: https://doi.org/10.1016/j.jhydrol.2022.127455. URL: https://www.sciencedirect.com/science/article/pii/S0022169422000300 (cit. on p. 25).

[26] R. Fleck, M.T. Westerhausen, N. Killingsworth, J. Ball, F.R. Torpy, and P.J. Irga. «The hydrological performance of a green roof in Sydney, Australia: A tale of two towers». In: *Building and Environment* 221 (2022), p. 109274. ISSN: 0360-1323. DOI: https://doi.org/10.1016/j.buildenv.2022.109274. URL: https://www.sciencedirect.com/science/article/pii/S0360132322005091 (cit. on p. 26).

[27] ARPA Piemonte. *Dati metoidrografici giornalieri*. https://webgis.arpa.piemonte.it/radar/open-scripts/richiesta_dati_gg_2024.php. Accessed: 2024-07-07. 2024 (cit. on p. 27).

[28] Centro Euro-Mediterraneo sui Cambiamenti Climatici (CMCC). *Climate Projections RCP85 Downscaled over Italy - Historical*. https://dds.cmcc.it/#/dataset/climate-projections-rcp85-downscaled-over-italy/historical. Accessed: 2024-09-07. 2023 (cit. on pp. 27, 47).

[29] Mario Raffa, Marianna Adinolfi, Alfredo Reder, Gian Franco Marras, Marco Mancini, Gabriella Scipione, Monia Santini, and Paola Mercogliano. «Very High Resolution Projections over Italy under different CMIP5 IPCC scenarios». In: *Scientific Data* 10.238 (2023). DOI: https://doi.org/10.1038/s41597-023-02144-9. eprint: https://onlinelibrary.wiley.com/doi/pdf/10.1002/hyp.9876. URL: https://www.nature.com/articles/s41597-023-02144-9#citeas (cit. on p. 28).

[30] M.B. Kirkham. «Chapter 28 - Potential Evapotranspiration». In: *Principles of Soil and Plant Water Relations (Second Edition)*. Ed. by M.B. Kirkham. Second Edition. Boston: Academic Press, 2014, pp. 501–514. ISBN: 978-0-12-420022-7. DOI: https://doi.org/10.1016/B978-0-12-420022-7.00028-8. URL: https://www.sciencedirect.com/science/article/pii/B9780124200227000288 (cit. on p. 34).

[31] R Rusnam and N R Yanti. «Potential Evapotranspiration uses Thornthwaite Method to the Water Balance in Padang City». In: *IOP Conf. Series: Earth and Environmental Science* 757 (2021), p. 012041. ISSN: 0301-4797. DOI: 10.1088/1755-1315/757/1/012041. URL: https://iopscience.iop.org/article/10.1088/1755-1315/757/1/012041/pdf (cit. on p. 34).

[32] Antonio Roberto Pereira and William Oregon Pruitt. «Adaptation of the Thornthwaite scheme for estimating daily reference evapotranspiration». In: *Agricultural Water Management* 66.3 (2004), pp. 251–257. ISSN: 0378-3774. DOI: https://doi.org/10.1016/j.agwat.2003.11.003. URL: https:

//www.sciencedirect.com/science/article/pii/S0378377403003196 (cit. on p. 35).

[33] F. Viola, D. Pumo, and L. V. Noto. «EHSM: a conceptual ecohydrological model for daily streamflow simulation». In: *Hydrological Processes* 28.9 (2014), pp. 3361–3372. DOI: https://doi.org/10.1002/hyp.9876. eprint: https://onlinelibrary.wiley.com/doi/pdf/10.1002/hyp.9876. URL: https://onlinelibrary.wiley.com/doi/abs/10.1002/hyp.9876 (cit. on pp. 36, 38, 64).

[34] Henny A.J. Van Lanen, Anne F. Van Loon, Niko Wanders, and Christel Prudhomme. «Chapter 9 - Process-based modelling». In: *Hydrological Drought (Second Edition)*. Ed. by Lena M. Tallaksen and Henny A.J. van Lanen. Second Edition. Elsevier, 2024, pp. 427–476. ISBN: 978-0-12-819082-1. DOI: https://doi.org/10.1016/B978-0-12-819082-1.00019-9. URL: https://www.sciencedirect.com/science/article/pii/B9780128190821000199 (cit. on p. 36).

[35] F. Laio, A. Porporato, L. Ridolfi, and I. Rodriguez-Iturbe. «Plants in water-controlled ecosystems: active role in hydrologic processes and response to water stress: II. Probabilistic soil moisture dynamics». In: *Advances in Water Resources* 24.7 (2001), pp. 707–723. ISSN: 0309-1708. DOI: https://doi.org/10.1016/S0309-1708(01)00005-7. URL: https://www.sciencedirect.com/science/article/pii/S0309170801000057 (cit. on p. 37).

[36] American Society of Agricultural and Biological Engineers. *Guidelines for Using Spreadsheets for Irrigation Data Management*. https://elibrary.asabe.org/data/pdf/7/sd2009/chap3_cdfiles/Guidelines_for_spreadsheets.pdf. [Online; accessed 25-Sep-2024]. 2009 (cit. on p. 37).